Technologies and Processes for the Advancement of Materials

Thermal processing

ISSUE FOCUS ///

VACUUM HEATING / CRYOGENICS

FINITE ELEMENT MODELING AND SIMULATION OF VACUUM BRAZING PROCESSES

ALSO ///

Improving cooling tunnel performance

JANUARY 2024
thermalprocessing.com

aichelin group

AFC HOLCROFT

industrial furnace solutions

Batch Integral Quench Furnaces and Endothermic Gas Generators "Built for Stock"

Leading the Industry with the Fastest Delivery Available

Supply chain interruptions don't have to derail your valuable heat treating production. When you need a new batch integral quench furnace or endothermic gas generator, AFC-Holcroft's Built for Stock equipment will shave months off typical delivery timeframes.

We're always building our industry-leading UBQ (Universal Batch Quench) furnaces and EZ™ Series Endo Gas Generators for off-the-shelf delivery, ready for expedited shipment. The same standard equipment AFC-Holcroft is known for, but pre-built to speed up typical delivery by months. There is no compromise in quality to get this fast delivery.

Built for Stock equipment gets you in production faster.

Talk to our Sales staff to find out more.

AFC-Holcroft Headquarters
Wixom, Michigan, USA
Phone: +1 248 624 8191

AFC-Holcroft Europe
Swiebodzin, Poland
Phone: +48 68 41 61 776

AFC-Holcroft Asia
Shanghai, P. R. China
Phone +86 21 5899 9100

www.afc-holcroft.com

CONTENTS ///

COVER PHOTO: SHUTTERSTOCK (2) / ILLUSTRATION BY RICK FRENNEA

DEPARTMENTS ///

JANUARY 2024 VOLUME 13 / NUMBER 1

UPDATE ///

New Products, Trends, Services & Developments

Q&A ///

RESOURCES ///

International Federation for Heat Treatment (IFHTSE)

Industrial Heating Equipment Association (IHEA)

METAL URGENCY ///

HOT SEAT ///

Thermal Processing is published monthly by Media Solutions, Inc., 266D Yeager Parkway Pelham, AL 35124. Phone (205) 380-1573 Fax (205) 380-1580 International subscription rates: $105.00 per year. Postage Paid at Pelham AL and at additional mailing offices. Printed in the USA. POSTMASTER: Send address changes to *Thermal Processing* magazine, P.O. Box 1210 Pelham AL 35124. Return undeliverable Canadian addresses to P.O. Box 503 RPO West Beaver Creek Richmond Hill, ON L4B4R6.

CUSTOM DESIGN HEAT RESISTANT CASTINGS AND FABRICATIONS

Wirco has been trusted for over 60 years to develop and manufacture high-temperature heat treatment tooling for numerous industries in the form of both castings and fabrications.

Wirco has capabilities to create any custom designed tooling of any shape and size along with specific fabrication techniques to help meet the needs for your process.

Wirco's serpentine trays are built to stay flat while providing ample strength under heavy loads. Our construction techniques allow for expansion and contraction during the heating and cooling process. Utilizing light weight construction, Wirco's serpentine trays will increase your part allowance by decreasing tooling weight. Wirco can custom design a tray of any size to fit your application.

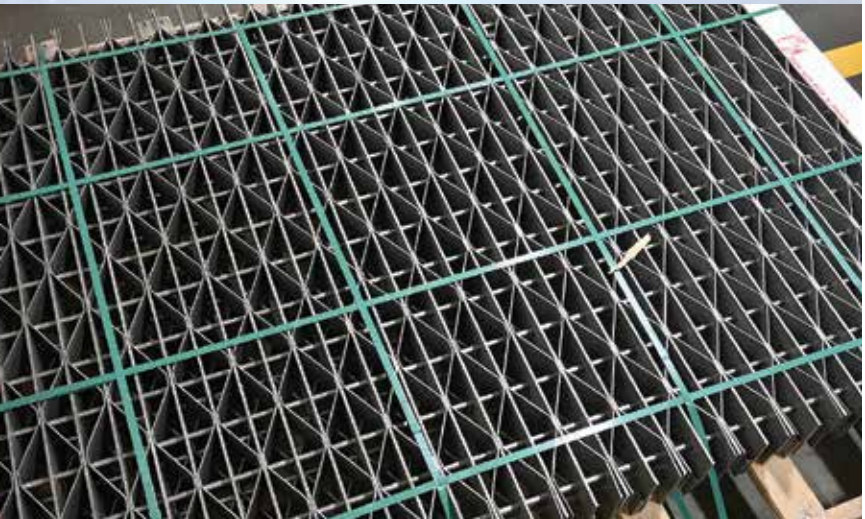

OUR GOAL

CREATE EXCELLENT PRODUCTS AND PARTNERSHIPS

- Fabricated Heat Treating Work Carriers
- Cast Heat Treating Work Carriers
- Heat Treatment Furnace Parts
- Steel Production Support
- Hyper Alloys Fabricated Products

CONTACT US

Sales@Wirco.com

800.348.2880

Partner with Wirco, your American-made engineered alloy solution.

FROM THE EDITOR ///

Leaping into 2024!

As we enter 2024, please make sure you stay quiet and don't make any sudden movements.

All kidding aside, we all have our fingers crossed that this year will bring some good things our way.

Ever since *Thermal Processing* began, we have always tried to confront the challenge head on of bringing you the best industrial heat-treat news, and this year should be no different. We will continue our promise to share all the latest facts and innovation about the heat-treating world.

And if you're traveling to some of the big trade shows scheduled in 2024, make sure you look for *Thermal Processing,* as we plan to participate in quite a few of them.

To get you primed for what's sure to be a stellar year for the industry, our first issue of the year takes a look at vacuum heating and cryogenics.

Our cover story looks at vacuum heating — specifically vacuum brazing. In the story, it takes a deep dive with a study that breaks down a new method of radiation and contact modeling developed to identify the most critical influencing factors of distortion for vacuum brazed assemblies with simulation.

This issue's second focus article is a case study on improving the cooling tunnel performance of an aluminum caster that upgraded some technology that increased the company's uptime by more than 50 percent.

Rounding out our focus articles is a story from Joseph E. Harmon with the Argonne National Laboratory. In his piece, he discusses a new center funded by the Department of Energy that will develop a cost-effective method for decarbonized manufacturing for steelmaking without a blast furnace.

After you digest those articles, make sure you check out what our columnists have cooked up for January as well. They are always sharing some fascinating information.

And since it is the first of the year, I will take this opportunity to remind all of you that I am always on the lookout for articles and other submissions. It's a great way to share your expertise while shining a spotlight on you and your company at the same time. Hit me up if you have an article idea.

Thanks again for helping us through 2023, and we look forward to making 2024 even better.

Happy New Year, and, as always, thanks for reading!

KENNETH CARTER, EDITOR
editor@thermalprocessing.com
(800) 366-2185 x204

CALL FOR ARTICLES Have a technical paper or other work with an educational angle? Let Thermal Processing publish it. Contact the editor, Kenneth Carter, at *editor@thermalprocessing.com* for how you can share your expertise with our readers.

Thermal processing

David C. Cooper
PUBLISHER

EDITORIAL

Kenneth Carter
EDITOR

Jennifer Jacobson
ASSOCIATE EDITOR

Joe Crowe
ASSOCIATE EDITOR | SOCIAL MEDIA

SALES

Dave Gomez
VICE PRESIDENT I SALES & MARKETING

Kendall DeVane
NATIONAL SALES MANAGER

Susan Heinauer
REGIONAL SALES MANAGER

CIRCULATION

Teresa Cooper
MANAGER

Jamie Willett
ASSISTANT

DESIGN

Rick Frennea
CREATIVE DIRECTOR

Michele Hall
GRAPHIC DESIGNER

CONTRIBUTING WRITERS

JOSEPH E. HARMON
TIM HENNING
D. SCOTT MACKENZIE
FINN ONTRUP
TRIRATNA SHRESTHA
JACKIE STOKES
WOLFGANG TILLMANN
CHRISTIAN TIMMER
LUKAS WOJARSKI

media solutions

PUBLISHED BY MEDIA SOLUTIONS, INC.
P. O. BOX 1987 • PELHAM, AL 35124
(800) 366-2185 • (205) 380-1580 FAX

David C. Cooper
PRESIDENT

Teresa Cooper
OPERATIONS

INDUSTRIAL HEATING EQUIPMENT ASSOCIATION IHEA

IFHTSE

Designed specifically to meet the brazing needs of North American heat-exchanger manufacturers, the Seco/Warwick Active Only® CAB furnace offers tremendous gains in both productivity and energy efficiency. (Courtesy: Seco/Warwick)

Seco/Warwick USA contracts for Active Only CAB Furnace

A manufacturer of HVAC systems has awarded Seco/Warwick's American subsidiary a contract for a new controlled atmosphere brazing (CAB) furnace. Designed specifically to meet the brazing needs of North American heat-exchanger manufacturers, the furnace offers tremendous gains in both productivity and energy efficiency.

The operating sequence of the Active Only® CAB furnace is divided into stages. These include loading, drying in the dryer, nitrogen purging in the purging chamber, heating and brazing in a proprietary convection chamber, pre-cooling in the cooling chamber with an air-jacket, and the final direct air cooling in the final cooling chamber.

The semi-continuous furnace system is designed to operate on a part-time basis. The furnace can be brought up to brazing temperature from ambient and conditioned with a proper atmosphere in a very short time. This semi-continuous system allows for variable heating and cooling rates, depending on indexing times. This furnace can braze the widest variety of heat exchangers when lower total production requirements are needed.

As a conveyor furnace with a semicontinuous through process, it is capable of brazing parts at significantly higher rates than its previous batch furnace.

"Their manufacturing line is not a smooth, even flow of identical parts," said Marcus Lord, managing director, Seco/Warwick USA. "Instead, part flow is intermittent and variable sizes. It is why we made the Active Only CAB furnace, to meet just such a demand."

The CAB furnace operates entirely on electricity, resulting in zero carbon emissions when powered by the region's renewable energy grid. This new furnace is anticipated to not only double production capacity but also lead to a tangible reduction in the plant's overall carbon footprint.

Not only will the furnace handle anything they currently produce, but the Active Only furnace is built to be versatile, which offers the manufacturer flexibility to braze whatever new heat exchangers they might offer in the future as well.

MORE INFO www.secowarwick.com

Dimas Ventura joins Ipsen as regional service manager

Ipsen has announced the hiring of an additional regional service manager to support their market share growth in the Western United States. Dimas Ventura comes to Ipsen with 18 years of experience in field service, most recently serving as a maintenance manager for Amazon.

Dimas Ventura

Long-tenured Ipsen West Coast service manager Vince Fitzgerald will turn his focus to the critical customer base in the high-density Southern California and Northern Mexico markets, while also providing guidance and support to Ventura during his transition.

"Vince will continue to offer his highly regarded support and expertise to our customers, which has been key to our ongoing success in this region," said Ipsen USA president and CEO Patrick McKenna. "With the growth we have achieved in the Western United States comes the need for additional resources."

Ipsen has an installed base of more than 500 furnaces in the Western United States that are supported by eight full-time field service engineers.

"The added support that Dimas brings to the region will ensure faster response times to our customers' service needs." said David Choate, Ipsen's director of service.

Ipsen has hired an additional seven field service engineers in North America in 2023, including one dedicated to atmosphere equipment, and is actively recruiting to fill several more field service positions to further expand their capacity in 2024 and beyond.

MORE INFO www.ipsenglobal.com

SEND US YOUR NEWS Companies wishing to submit materials for inclusion in Thermal Processing's Update section should contact the editor, Kenneth Carter, at editor@thermalprocessing.com. Releases accompanied by color images will be given first consideration.

E-Z Sonic™ tapered ultrasonic inserts are machined out of brass and are available in single and double-vane lengths for maximum design flexibility. (Courtesy: E-Z Sonic)

E-Z Lok introduces ultrasonic inserts and heat staking kits

E-Z Lok, a leading manufacturer and master distributor of threaded inserts for metal, plastic, and wood is now offering E-Z Sonic™ with threaded insert assortment kits.

E-Z Sonic inserts are designed for post-molding installation in thermoplastic materials such as acrylic, polypropylene, and PVC. Machined out of high-quality brass and available with both inch and metric threads, these inserts are durable enough for the toughest environments and versatile enough to meet the needs of any application. Designs include tapered and straight that can be installed either with an ultrasonic horn or a heat driver. Additional features are superior torque and pull-out resistance, inch or metric threads, tapered design in single and double vane, and straight design in flush or flanged configuration.

Straight inserts provide superior torque and pull-out resistance, while allowing for thinner boss walls. Flush inserts allow for installation even with or below the material surface. Flanged inserts are ideal for electrical connections or for additional pull-out resistance in reverse installations. Furthermore, E-Z Sonic straight threaded ultrasonic inserts feature a lead-in pilot to facilitate installation. Machined out of brass, the inserts are available with internal threads from two inches to 3/8 inches.

Tapered inserts are designed to reduce installation time, particularly in production runs, while maintaining outstanding performance characteristics. E-Z Sonic tapered ultrasonic inserts are machined out of brass and are available in single and double-vane lengths for maximum design flexibility. Internal threads from two to 3/8 inches and 2.5 mm to six mm are available.

Besides being ideal for post-molding installation in thermoplastics, the heat staking threaded insert assortment kits quickly add machine threads to 3D printed parts and prototypes. Design engineers and hobbyists alike will find value in the variety of thread options available in the kits. Threaded inserts in the kits are available in tapered and straight designs, with imperial and metric threads. Each kit includes 200 inserts and five installation tips for use with a soldering iron.

MORE INFO www.ezlok.com

Vulcan Green Steel orders DRI plant from Tenova, Danieli

Vulcan Green Steel, a new established company of Jindal Steel Group, relied on ENERGIRON® for its new hydrogen-ready direct reduction plant in Duqm, in the Al Wusta Governorate in the Sultanate of Oman. ENERGIRON is the DRI technology jointly developed by Tenova and Danieli that will feed a new electric steelmaking complex conceived as a hub for green steel production in the country.

ENERGIRON is H2-ready and allows use of natural gas as a reducing agent with the possibility to mix it with up to 100 percent hydrogen, according to hydrogen availability. The new ENERGIRON zero-reformer DR plant will produce 2.5-Mtpy of direct reduction ores and will start operation with natural gas feed, increasing the percentage of hydrogen in blend as hydrogen becomes available on site.

The single-module will hot charge an electric arc furnace (EAF) with a temperature over 600°C, allowing significant energy savings for the steelmaking process. The plant

A new 2.5-Mtpy ENERGIRON® zero-reformer plant will be installed in Oman. (Courtesy: Tenova)

will also be able to produce hot briquetted iron (HBI) for storage or export purposes.

The ENERGIRON technology has the capability to capture CO2 from the process and use it for other applications, which will further reduce the overall plant emissions and, together with the EAF, bring the green steel hub closer to achieving carbon-neutrality. Additionally, it will also provide an additional revenue stream for the plant operations.

The completion of the DRI Plant in Duqm site is scheduled for 2026.

"Vulcan Green Steel, led by Jindal Steel Group, represents our flagship initiative to lead the green transition for the global steel industry," said D.K. Saraogi, projects director, Vulcan Green Steel. "Each of us in the steel industry has to do our part to decarbonize: our investment in Duqm is a visionary project set to become the largest green hydrogen ready steel plant globally."

"As a sustainable technology supplier for the steel sector, Tenova is privileged to be part of this green hydrogen-ready steel plant by suppling our flexible and innovative ENERGIRON DRI technology which nowadays has become a key pillar for the decarbonization targets of our industry as we aim for a cleaner world," said Jorge Martinez, Tenova HYL commercial director. "Our collaboration with Vulcan Green Steel embodies the strong commitment of ENERGIRON for greener steel production."

MORE INFO www.tenova.com

Abbott Furnace announces 2024 symposium dates

Join some of the world's experts in the brazing of carbon steel, stainless steel, brass, and aluminum when Abbott's U.S. Symposium takes place May 7-9, 2024, in Nashville, Tennessee.

Abbott's Mexico Symposium will take place November 5-7, 2024, in Monterrey, Mexico. More details and registration information will come later in 2024.

Abbott Furnace Company's two-and-a-half-day symposiums cover brazing fundamentals, filler metals, joint design, troubleshooting, and the new AIAG CQI-29 – Brazing Special Process Assessment.

The symposiums are ideal for brazing engineers, maintenance personnel, product designers, and anyone involved in the production of brazed components. They are an excellent opportunity for beginners and experienced employees to learn from the experts in the areas of:

- Furnace brazing CQI-29.
- Continuous furnace maintenance atmosphere control.
- Wire mesh belts furnace optimization furnace safety troubleshooting.
- Filler metals fundamentals joint design.
- Part preparation and cleaning.

Along with an opportunity to hear from the experts in the industry, attendees will be able to interact individually with the lecturers to address more specific questions and issues. They can bring in problem parts and speak with one of the experts who can troubleshoot what is happening in the manufacturing process that is causing the issue.

MORE INFO www.abbottfurnace.com

Manufacturing Talk Radio podcast celebrates 10 years

Manufacturing Talk Radio, a podcast launched on November 4, 2013, has reached its tenth broadcasting anniversary as the most-viewed manufacturing podcast.

The podcast has 5,000 to 25,000 views per episode on YouTube, plus thousands of additional listeners on Apple podcasts, Spotify, Google Play, iHeartRadio, and other podcast apps. The talk show format is geared to all executive and employee levels within manufacturing, including supply chain partners and customers of the more than 600,000 manufacturers across the United States. The weekly podcast is popular in many other countries as the voice of manufacturing globally.

"When we launched Manufacturing Talk Radio, it was a marketing tool to help promote sponsors of the show," said Lewis A. Weiss, founder of the podcast. "All Metals & Forge Group was the first sponsor and remains a sponsor today. But the podcast took on a life of its own as notable people

Manufacturing Talk Radio is a weekly podcast hosted by Lew Weiss and Tim Grady, who create casual conversations with guests that are in-depth, insightful, and informative to educate and often entertain any listener working in or aligned with the manufacturing industry. (Courtesy: Manufacturing Talk Radio)

from the industry, academia, federal, state, and local elected officials, and directors of industry associations began to take notice and appear as guests on the show. One of its key attributes is that it is not a 'gotcha' interview. It is a friendly conversation to help people in the myriad of manufacturing positions make more informed decisions and keep pace with an industry filled with digital disruption and rapid evolution."

When the Manufacturing Talk Radio podcast launched, its first guest was Brad Holcomb, committee chair for the Institute of Supply Management's Manufacturing Report on Business®. He went beyond the headline Purchasing Manager's Index number and shared ISM's understanding of the subindexes that make up that top-line figure. The manufacturing subindexes are new orders, production, employment, supplier deliveries, and inventories in production plants. Each month, ISM continues to present in-depth discussion of the Manufacturing Report on Business with Tim Fiore, the Service Report on Business ® with Anthony Nieves, and the Semi-Annual Forecast released in May and December. The ISM Manufacturing and Services Indexes are a monthly gauge of the level of economic activity in the U.S. manufacturing and services sectors versus the previous month.

"The detail in the subindexes gives manufacturers and service providers a good read on the recent past ebb and flow of the industry as a whole, and their sector in particular, and has proved to be a potential forecasting tool when the data is compared to previous expansion and recession cycles," said Weiss. "We are grateful to the ISM for their continued involvement with us over this exciting 10-year growth period.

"Our mission has been, and continues to be, to share information that manufacturers and service companies can use to add to discussions within their own operations to make better-informed decisions," Weiss said.

"While we have fun doing it, with some occasional levity in our discussions with guests, we are intensely careful to convey accurate and reliable information without political positions overriding reason. Manufacturing does not like uncertainty, and we are in an unfortunate cycle of much uncertainty, caught between forecasts or recession and expansion, inflation and high employment, inverted bond yields and consumer uncertainty, and other factors that make 2023 and 2024 a kaleidoscope of unpredictable possibilities. This is why we continue to produce the Manufacturing Talk Radio Podcast and its more specialized podcasts, including The Flagship Report with noted economist Dr. Chris Kuehl, Manufacturing Think Tank with Cliff Waldman, Moser on Manufacturing with Harry Mosser on Reshoring, and Hazard Girls with Emily Soloby and women discussing their roles in non-tradition fields," he said.

"To further enhance the message, we also publish a free monthly ezine called Manufacturing Outlook that dovetails with Manufacturing Talk Radio by discussing the outlook for various manufacturing sectors, and how economies around the world are performing, since imports and exports are a major component of the GDP of many countries. Between Manufacturing Talk Radio and Manufacturing Outlook, we present information that can be used worldwide," said Weiss, who is also the publisher of Manufacturing Outlook.

MORE INFO www.mfgtalkradio.com

Nord Drivesystems manager receives AGMA award

Hani Almoghrabi, product manager for Nord's large industrial drives, accepted an award for his contributions to a published document regarding thermal capacity of gear units.

This fall, the American Gear Manufacturers Association (AGMA) presented various awards during the 2023 Fall Technical Meeting (FTM) awards luncheon in Detroit, Michigan. Along with the Chairperson's Award, awards were presented to AGMA technical committee members who have published a document within the last year.

Almoghrabi, product manager for MAXXDRIVE Industrial Gear Units at Nord Drivesystems, was recognized for his contribution toward publishing AGMA 947-A23, Gear Reducers – Thermal Capacity. Ten other members of the AGMA Drives for Industrial Applications Committee also accepted awards for their work on the piece.

"It was a pleasure working alongside my colleagues on the AGMA Enclosed Gear Committee to publish the AGMA 947-A23 Gear Reducers-Thermal Capacity information sheet," said Almoghrabi. "We hope it will become an informative resource for the gear industry."

The published document uses an analytical heat balance model as a means of calculating the thermal transmittable power of a gear unit lubricated with mineral oil. The calculation is based on the standard conditions of 25°C (77°F) maximum ambient temperature and 95°C (203°F) maximum oil sump temperature in a large indoor space but also includes modifiers for calculation in other conditions. The first draft of AGMA 947-A23 was created in April 2019 and approved by the Technical Division Executive Committee in June 2023.

NORD product manager for industrial drives Hani Almoghrabi with the award for his contributions to the published AGMA document on thermal capacity of gear reducers. (Courtesy: Nord Drivesystems)

MORE INFO www.nord.com

Retech, a division of Seco/Warwick Group, announced its recent membership with America Makes, the National Additive Manufacturing Innovation Institute. (Courtesy: Seco/Warwick)

Retech joins America Makes to help advance AM

Retech, a division of Seco/Warwick Group, announced its recent membership with America Makes, the National Additive Manufacturing Innovation Institute, joining them in their mission to accelerate the adoption of additive manufacturing by convening, coordinating, and catalyzing the AM industry to help advance U.S. manufacturing competitiveness and security.

America Makes is the nation's leading public-private partnership for additive manufacturing (AM) technology and education. America Makes members from industry, academia, government, workforce, and economic development organizations, work together to accelerate the adoption of AM and the nation's global manufacturing competitiveness. Founded in 2012 as the Department of Defense's national manufacturing innovation institute for AM and first of the Manufacturing USA network, America Makes is based in Youngstown, Ohio, and managed by the not-for-profit National Center for Defense Manufacturing and Machining (NCDMM).

"Healthy competition means joining the same sports league," said Earl Good, Retech managing director/president. "There is still competition, but it is organized around common goals, which drives everyone to improve. America Makes brings that to additive manufacturing."

The Retech team looks forward to contributing their 60 years of accumulated wisdom and experience in vacuum metallurgy, including more than twenty years of experience manufacturing vacuum atomization technology, with their additive manufacturing colleagues in industry, government, and academia.

Much like the additive manufacturing process itself, the whole is greater than the sum of its parts. Aggregating many small organizations and individuals together is more functional once they are bonded together to form a common purpose. The opportunities for networking and collaboration in support of the America Makes mission will benefit the entire U.S. domestic AM industry, Retech included.

"We see this membership as having many overall benefits for Retech, for example, the time and effort Retech invests in strengthening academic programs in AM, will pay dividends in the form of more graduates with the skills we are looking for and potentially create more uses for our vacuum melting equipment," Good said.

MORE INFO www.secowarwick.com

IFHTSE seeks abstracts for World Congress 2024

The ASM Heat Treating Society (HTS) and the International Federation for Heat Treatment and Surface Engineering (IFHTSE) announced the 29th IFHTSE World Congress, a pinnacle global event focused on advancing heat treatment and surface engineering.

Themed "Innovations in Heat Treatment and Surface Engineering for a Sustainable Future," this congress spotlights the pivotal role of these technologies in shaping sustainability in heat treatment. It will be held September 30–October 3, 2024, in Cleveland, Ohio, with IMAT and ASM's annual meeting.

They are encouraging abstract submissions of 150–200 words or less to help shape the technical program.

Deadlines for IFHTSE Congress 2024:

» Submission deadline: January 26, 2024.

» Author notifications of acceptance: March 29, 2024.

» First draft of manuscript due: May 17, 2024.

» Editor feedback to authors: June 14, 2024.

» Final manuscripts due: June 28, 2024.

Abstracts will be solicited for (but not limited to) the following topical programs:

» Additive manufacturing.

» Applied energy.

» Applied technology / processes and applications: Including energy consumption and efficiency; quality control.

» Atmosphere technology and surface engineering.

» Automotive lightweighting.

» Cryogenic treatment.

» Heat treating: Including green heat treating / low carbon; heat treating of dissimilar material structures; heat treatment of EV components; induction heat treating; new trends in global heat treatment / new methods; quenching technologies and distortion.

» Surface engineering: carburizing, nitriding, engineered coatings.

» Industry 4.0 process controls.

» Materials durability / mechanical testing / non-destructive testing.

» Microstructural development / characterization.

» Other materials: Including e-steel (motor components, magnets, etc.), amorphous metals; non-ferrous alloys; semiconductors and compound semiconductors (SiC, GaN).

» Residual stress: measurement and prediction.

» Simulation and modeling: Material property prediction (JMATPro/Thermocalc/Calphad); process simulation (CFD/FEA); materials informatics, and ICME approaches.

» Thermal processing: High temperature material, non-metals.

» Vacuum processes and technology.

MORE INFO www.asminternational.org

Hexonic orders Seco/Warwick Vector vacuum furnace

Hexonic Ltd., a European manufacturer of heat exchangers who has been providing advanced and reliable heat exchanger technologies for various industries for 35 years, purchased a Vector vacuum furnace from Seco/Warwick. The solution will be used mainly for brazing heat exchangers.

The furnace was covered by the fast delivery program, so the implementation was extremely fast. The furnace has been adapted to Hexonic's specific expectations regarding high vacuum,and process cleanliness during soldering.

Metal heat-treatment furnaces are complex solutions which have many options for modifications. Often, the Partner's specific needs require a special solution design meeting these expectations.

"Seco/Warwick is one of a few manufacturers who have developed a strategy that allows furnaces to be quickly modified in order to meet specific needs based on a standard product portfolio," said Sławomir Woźniak, CEO of the Seco/Warwick Group. "This means faster order execution and, consequently, increased profits resulting from its implementation at the Partner's machinery park."

"This is our fourth delivery to Hexonic," said Maciej Korecki, vice president of the Seco/Warwick Vacuum Segment. "It is unique because we used a furnace from the quick delivery program, which was built with express implementation in mind. We have adapted it to Hexonic's needs and guidelines so that it meets all key criteria. We can apply a similar procedure to any standard product. For our customers this means a significant reduction in delivery time and greater furnace availability."

The furnace purchased by Hexonic is based on a standard solution with a working space of 900x800x1,500 mm, graphite insulation, graphite heating elements, and specialized nozzles equipped with radiators, reducing the solder deposition. This fits perfectly into the customer's specific needs regarding soldering processes. The round heating chamber allows the user to load oversized elements.

The characteristic features of this structure include a high vacuum system that can achieve a high working vacuum of 10-5 mbar, convection heating up to 750°C (a system which improves the heat transfer efficiency when heating at lower temperatures), and a dew point sensor (a system which solves one of heat treatment's very critical requirements by preventing water vapor condensation which, in turn, causes load surface oxidation).

A Vector vacuum furnace purchased from Seco/Warwick by a European manufacturer of heat exchangers will be used mainly for brazing heat exchangers. (Courtesy: Seco/Warwick)

The use of an efficient cooling system with a pressure of six bar allows the system to significantly shorten the load cooling time, and thus significantly increase the furnace productivity.

"The Vector furnace will streamline and increase the soldering processing capacity, and improve the process economics, through energy savings and the graphite chamber efficiency, as well as the process cleanliness and velocity," said Jędrzej Malinowski, sales manager of the Seco/Warwick vacuum furnace team. "It is a furnace based on our proven solution, with specially redesigned nozzles and power feedthroughs enabling an effective soldering process and ensuring reliable furnace operation in industrial conditions. We are a major manufacturer of equipment for metal heat treatment, so we can afford to build both standard equipment and special orders. We have many solutions in an advanced production cycle which we can quickly deliver to the customer. Importantly, we can modify each of them to meet specific production expectations."

Aluminum heat exchanger brazing can be performed either in a protective atmosphere (CAB technology) or in vacuum (VAB technology). In the case of stainless exchangers, vacuum technologies are used. Seco/Warwick has extensive experience supplying these technologies to heat exchanger manufacturers from many industries.

"We have been supplying specialized heat exchangers for various industries for over 35 years," said Wojciech Zygmunt, Hexonic operations director. "We work for customers almost all over the world. Heat exchangers require high-quality joints, which we can achieve using brazing technology. We are cooperating with Seco/Warwick for the fourth time, which in itself should be an excellent recommendation."

MORE INFO www.secowarwick.com

Tenova strengthens cooperation with Tata Steel Group

Tenova was awarded a new order for a tinplate coating line and tinplate double reduction mill by the Tinplate Company of India Ltd. for its new tinplate complex at the Jamshedpur plant in Jharkhand, India.

Tenova is a leading company specialized in sustainable solutions for the metals and mining industries. The Tinplate Company of India Ltd. is a subsidiary of Tata Steel.

The tinplate coating line (TCL) includes an independent pre-tinning section with sulfuric acid for iron control in the electrolyte solution and an advance tinplate coat-

ing control close loop to achieve the best strip coating quality and stability. Superior efficiency in tinplate coating is guaranteed by the IGBT AFE rectifier technology that, moreover, allows the lowest electrical consumption of the line. The line also has the fastest tinplate coating process speed thanks to the cut-to-edge tinplate coating design, which allows to achieve the largest production capability.

The tinplate double reduction mill (TDRM) plays a key role in obtaining a combination of ultra-light strip gauge and required hardness. This mill is equipped with advanced technology, including high-performance automatic gauge control (AGC) cylinders, automatic flatness control (AFC) system, a roughness control system, and a dedicated reduction control for double reduced (DR) tin plate.

"We are very proud to have been selected as the main technological partner for Tata Group tinplate expansion," said Giuseppe Zanzi, chief representative officer, South East Asia and Oceania at Tenova. "Thanks to our solutions, Tata will be able to achieve a sustainable production based on low electrical consumption and very large production capacity. In a short time-span, this is already the third tinplate coating line and tinplate double reduction mill project awarded to Tenova, following contracts with JSW Steel, India, and Tosyali Toyo, Turkey. The successful combination of these two Tenova technologies underlines our notable experience, with more than 30 installations worldwide, as well as our reliability in the field of the tinplate coating process."

Tinplate Company of India Ltd., a subsidiary of Tata Steel, awarded Tenova contract for new tinplate coating line and tinplate double reduction mill. (Courtesy: Tenova)

"This order testifies the trust Tata Steel has placed in us," said Amitabh Nandi, Tenova Technologies Pvt. Ltd. managing director. "As the managing director of Tenova India, it's truly satisfying to witness our achievement align with our vision of forging a more sustainable future for the steel industry."

MORE INFO www.tenova.com

Stocky, Fechte-Heinen elected to IFHTSE Executive Council

Christophe Stocky recently was elected to be a member of the IFHTSE Executive Council in Yokohama at the recent IFHTSE Congress. He is a graduate of Mechanical Engineering from Karlsruhe Institute of Technology and Ecole Nationale Supérieure des Arts & Métiers.

He is the technical person responsible at the R&D center of ABS, an Italian steel maker and based in Metz. Stocky is an active member of the French Heat Treatment Association, A3TS, and is serving on the Executive Committee of A3TS.

Prof. Dr. Ing. Rainer Fechte-Heinen was recently elected to be a member of the Executive Council of IFHTSE in Yokohama at the IFHTSE Congress. He is executive director of Leibniz-Institut für Werkstofforientierte Technologien – IWT, and is the Department Chairman of Materials Engineering in Bremen Germany.

Previously he was the head of Product Development: Technology and Innovation at ThyssenKrupp Steel Europe AG, Duisburg, Germany.

Fechte-Heinen has been a member of the Governing Council of IFHTSE since 2020. He is a member of the German Heat Treatment Society, "Arbeitsgemeinschaft W rmebehandlung und Werkstofftechnik e.V." (AWT), and is the editor in chief of *HTM – Journal of Heat Treatment and Materials* since 2020.

Christophe Stocky

Rainer Fechte-Heinen

CONFERENCE UPDATES

4th Mediterranean Conference on Heat Treatment and Surface Engineering (MCHTSE 2024) | April 17-19, 2024

This conference will be held together with the 5th International Conference on Thermal Process Modeling and Simulation (5th ICTPMS), in Lecce, Italy.

The conferences aim to provide a forum where engineers, scientists, researchers, and production managers can review and discuss fundamentals, new challenges, recent progress, and emerging topics in the fields of advanced heat treatment and surface engineering technology.

TPMS-5 aims at covering all aspects of modeling and simulation of thermal processes.

The extended deadline for abstracts is January 15, 2024

More info: www.aimnet.it/eng/manifestazione.php?id=789&idc=4

2nd Bosphorus International Heat Treatment Symposium | April 25-26, 2024

BHTS'2024 - 2nd Bosphorus International Heat Treatment Symposium will be in Istanbul, Türkiye, at the Halic Congress Center, in cooperation with MISAD-Heat Treatment Industrialists Association and METEM-UCTEA Chamber of Metallurgical and Materials Engineers' Training Center.

With the scope of this symposium, a space will be created where the challenges in advanced heat treatment technologies, current R&D studies, new developments, and different ideas will be discussed. Within this framework, local, foreign, and international companies that want to exhibit their products, services, and exemplary applications to support them as participants are invited. The symposium is in Turkish and English. Turkish-English simultaneous translation will be provided in all sessions.

Deadline for Papers: January 19, 2024.

More info: www.bhtsheat.com/en

29th IFHTSE Congress | September 30-October 3, 2024

The ASM Heat Treating Society (HTS) and the International Federation for Heat Treatment and Surface Engineering (IFHTSE) will present the 29th IFHTSE World Congress, a premier global event dedicated to advancing the fields of heat treatment and surface engineering. Co-located with ASM's Annual Meeting, IMAT 2024, the congress will be in Cleveland, Ohio.

The 2024 IFHTSE World Congress revolves around the theme "Innovations in Heat Treatment and Surface Engineering for a Sustainable Future." Emphasizing the critical role of these technologies in shaping a sustainable world, the event will explore the latest developments, breakthroughs, and practices that can enhance the

efficiency, performance, and environmental impact of heat treatment and surface engineering processes. In addition, traditional heat-treating topics will be offered.

IMPORTANT DATES

- **Submission deadline:** January 26, 2024.
- **Author notifications of acceptance:** March 29, 2024.
- **First draft of manuscript due:** May 17, 2024.
- **Editor feedback to authors:** June 14, 2024.
- **Final manuscripts due:** June 28, 2024.

More info: www.asminternational.org/ifhtse-congress

SPOTLIGHT ON MEMBERS

University of Malta

Lying at the cross-roads of the Mediterranean, UM has been, over its 400-year history, the hub for international academic exchange on the island. UM is the leading higher education institution in Malta, and its structures are in line with the Bologna Process and the European Higher Education area. More than 24,000 students are enrolled in undergraduate and graduate levels.

Today UM is composed of 14 faculties, 14 interdisciplinary institutes and centers, three schools, and a junior college. In addition to the main campus situated at Msida, there are three other campuses: Valletta, Marsaxlokk, and Gozo. The language of instruction is English.

IFHTSE is a federation of organizations not individuals. There are three groups of members: scientific or technical societies and associations, universities and registered research institutes, and companies.

IFHTSE 2024 EVENTS

APRIL 17–19, 2024

4th Mediterranean Conference on Heat Treatment and Surface Engineering (MCHTSE 2024)

Lecce, Italy | www.aimnet.it/eng/manifestazione.php?id=788&idc=4

APRIL 17–19, 2024

5th International Conference on Thermal Process Modeling and Simulation (5th ICTPMS)

Lecce, Italy | www.aimnet.it/eng/manifestazione.php?id=789&idc=4

APRIL 25–26, 2024

2nd Bosphorus International Heat Treatment Symposium

Istanbul, Turkey | www.bhtsheat.com/en

MAY 6–8, 2024

3rd QDE - International Conference on Quenching and Distortion Engineering

Vancouver, Canada

SEPTEMBER 30-OCTOBER 3, 2024

29th IFHTSE Congress

Cleveland, Ohio | with IMAT and ASM's annual meeting

For details on IFHTSE events, go to www.ifhtse.org/events

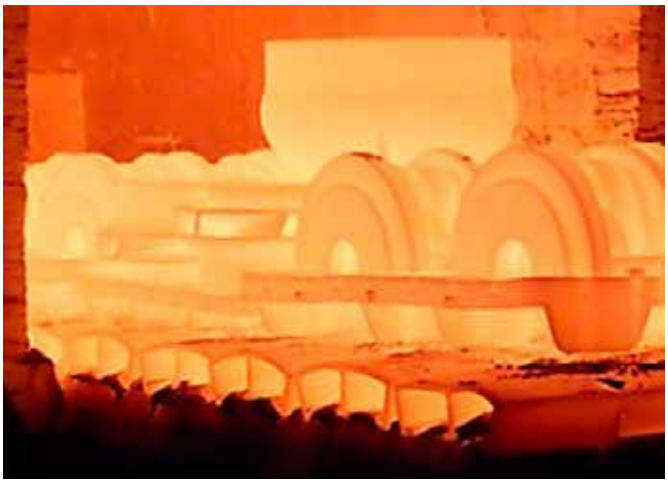

IFHTSE LEADERSHIP

EXECUTIVE COMMITTEE

Prof. Masahiro Okumiya | President
Toyota Technological Institute | Japan

Prof. Masahiro Okumiya | Past President
Toyota Technological Institute | Japan

Dr. Lesley Frame | Vice President
University of Connecticut | USA

Dr. Stefan Hock | Secretary General
IFHTSE | Italy

Dr. Imre Felde | Treasurer
Óbuda University | Hungary

OTHER MEMBERS

Prof. Rafael Colas | Universidad Autónoma de Nueva Leon | Mexico
Prof. Jianfeng Gu | Shanghai Jiao Tong University | China
Dr. Patrick Jacquot | Bodycote Belgium, France, Italy | France
Bernard Kuntzmann | Listemann AG | Switzerland
Dr. Scott Mackenzie | Quaker Houghton Inc | USA
Prof. Larisa Petrova | MADI University | Russia
Prof. Reinhold Schneider | Univ. of Appl. Sciences Upper Austria | Austria
Prof. Marcel Somers | Technical University of Denmark | Denmark
Prof. Mufu Yan | Harbin Institute of Technology | China

ONLINE www.ifhtse.org | **EMAIL** info@ifhtse.org

Hydrogen basics for industrial burners

Because burning hydrogen produces no carbon emissions, it provides a promising option for industry to reduce carbon emissions.

By BRIAN KELLY and JEFF RAFTER

Modern concerns for sustainable manufacturing are driving significant interest and investment in hydrogen as an industrial fuel. Because burning hydrogen produces no carbon emissions, it provides a promising option for industry to reduce carbon emissions. Burning hydrogen for industrial applications has been done for over a century, but only in selected industries with a ready source of hydrogen.

The science of burning hydrogen is well known, but converting to the fuel does not come without some risks and design considerations. This article will explain hydrogen basics and explore some concerns to be aware of in using the fuel.

HYDROGEN AS A FUEL

When hydrogen is produced using a renewable energy source, it results in being a CO_2 neutral form of fuel.

When natural gas is burned (assuming for simplicity that it is 100% CH_4) you produce CO_2, water vapor, and energy.

$$CH_4 + 2\ O_2 \longrightarrow CO_2 + 2\ H_2O + \text{energy}$$

When you burn 100% hydrogen, there is only water vapor and energy that results.

$$2\ H_2 + O_2 \longrightarrow 2\ H_2O + \text{energy}$$

So, hydrogen as a fuel source is attractive in being able to reduce or eliminate the carbon produced by thermal processes.

HYDROGEN COMBUSTION CHARACTERISTICS

- The H atom is the lightest and smallest element; it is eight times lighter than natural gas.
- It is colorless, odorless, and tasteless.
- The H_2 flame burns about eight times as fast as natural gas and with a higher flame temperature (approximately 400°F hotter than natural gas)
- H_2 is extremely flammable with a very wide flammability range in air (LEL to UEL (vol%) of 4-77) compared to natural gas at (5-15%).
- 15 times lower spark energy is needed to ignite H_2 than natural gas.
- The heating value by volume is 3-3.5 times less than commercially available natural gases.

BURNER AND SYSTEM CONSIDERATIONS

Hydrogen looks to be very suited as a fuel in combustion processes being more flammable and requiring less energy to ignite. However, burner designs vary widely to accommodate process requirements such as flame shape/velocity, emissions, efficiency, turndown, etc. So, what are some of the critical factors when considering H_2? For those, we look at burners and their systems:

Materials of construction: Burner materials of construction will need to be examined and often upgraded to accommodate increasing flame temperatures with increasing percentages of H_2 in natural gas up to 100%.

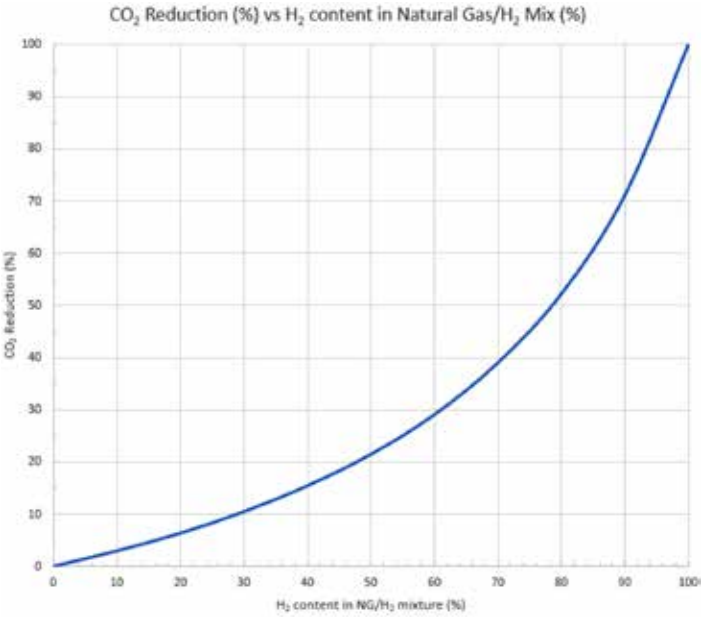

Figure 1

Burner design and selection: The method of air/fuel mixing design often will dictate how an existing burner design will react to the introduction of H_2 as the fuel source. Some burner designs require little or no change to be able to burn up to 100% H_2; however, burner designs using partial or full premix and/or high swirl are challenging, if not impossible, with the high flame speed of H_2.

If any degree of H_2 premix is intended with a burner application, be aware the very high flammability nature of hydrogen premix may require the use of additional equipment such as flashback arrestors or blow outs similar to high pressure natural gas premix.

Overall, do not assume H_2 can be used in any burner. Due to the nature of the fuel, always consult with equipment suppliers to determine if hydrogen fuel in a burner for your application is recommended and what, if any, changes are required.

Flame detection: UV sensors have been applied with H_2/gas mixtures up to 100% H_2 with no issue sensing the flame. Flame rod (ionization), flame rectification will become weaker as the percentage of H_2 in the gas becomes higher. Above 80-90% H_2 in the gas mixture, UV flame detection is recommended.

Gas pressure: To maintain the same thermal input, a burner will need higher gas pressure burning H_2 vs. natural gas since the heating value of H_2 by volume is about a third of natural gas. This pressure of course varies if you are burning H_2/Natural Gas blends.

Stoichiometric air required for combustion: General rule of thumb for natural gas combustion is a stoichiometric air/fuel ratio of about 10:1, so 10 cubic feet of air is required for every one cubic foot of natural gas burned. The approximate stoichiometric air/fuel ratio for hydrogen is 2.4:1, so 2.4 cubic feet of air is required for every one cubic foot of hydrogen burned. If we need 3.5 times the volume H_2 to equal the given heat input using natural gas, then for equal heat release we would need $3.5 ft^3$ H_2 * 2.4 ft^3 air/ft^3 H_2 = $8.4 ft^3$ air for hydrogen. Or we need about 85% of the air volume for pure H_2 combustion versus natural gas combustion.

If you intend to fire varying percentages of natural gas/H_2 blends, or at times 100% of either fuel, then depending on your application, you may have to look at your burner control system and ability to adapt air fuel ratio (excess air), if that is important in your process or for your product.

Fuel Safety trains and control valves: When you consider blending or running your system on a blend or up to 100% H_2, then the safety and control equipment and materials of construction that are part of that system need to be suitable for H_2 service. The majority of our process heating systems runs at low fuel temperatures and pressures, so hydrogen embrittlement should not be a concern. For your safety and control devices, you should confirm their suitability for hydrogen service.

Due to the very low heating value of hydrogen, a much higher volume of the fuel must be fed to a burner for a similar total heat input. As such, fuel handling components like regulators, control valves, mixers, and shut off valves may have to be replaced or added to allow the larger volume of fuel to be fed to burner at a given supply pressure.

CO_2 reduction with natural gas/H_2 blending: If you consider the blending of hydrogen with natural gas to start reducing CO_2 emission, be aware that the percentage of hydrogen in the mixture is not a direct correlation to the amount of CO_2 reduction in the combustion products. This is a result of hydrogen's lower heating value and very low density. You can see in the Figure 1 that to realize a 50% reduction in CO2 emissions, you need almost 80% hydrogen in your hydrogen/natural gas blend.

Emissions: The impact of H_2 on NOx will be highly influenced by the burner design. We have seen increases in volumetric (ppm) NOx levels as the percentage of H_2 increases in the gas mixture resulting from the increase in flame temperature. But this volumetric reference/measurement can be misleading because of the change in volume of products of combustion and other corrections when firing H_2. So volumetric comparison (e.g., ppm) should be avoided and a mass/unit energy is recommended to compare NOx from natural gas vs H_2 combustion.

EXAMPLES

NOx (Natural Gas)

50ppm (corr. to 3% O_2) = 0.060 lbs/MM Btu

NOx (H2)

50ppm (corr. to 3% O_2) = 0.041 lbs/MM Btu

So, to equal the same lbs/MM Btu with H_2 as with natural gas the conversion is:

0.060 lbs/MM Btu = 73ppm (corr. to 3% O_2)

So be aware of this when environmental agencies and regulations are of concern.

ABOUT THE AUTHORS

Brian Kelly is with Honeywell Thermal Solutions and is IHEA president. Jeff Rafter is with Selas Heat Technology and is IHEA vice president.

TRIRATNA SHRESTHA
MANAGER OF METALLOGRAPHIC LABORATORY AND CENTRAL COATINGS LABORATORY /// METCUT RESEARCH INC.

Pay attention to development, application, manufacturing, and quality control to ensure best results.

Gas turbine coating's life cycle

Gas turbines on land, air, and at sea experience some extreme environments, such as high airflow, pressure, and temperature. Engines intake air from outside and compress it to increase pressure ratio. Burning of fuel occurs in the combustor, where nozzles spray fuel to combust with compressed air uniformly to generate maximum heat. This process sees maximum temperature rise in the system, which puts limitations on material selection in terms of high temperature deformation, high temperature corrosion, and fatigue. The air intake and compression expose materials to erosion and wear. To protect engine parts from physical, chemical, and thermal damage, engine parts are coated with a variety of coatings. Furthermore, these coatings assist in increasing operating temperatures, thus increasing fuel efficiency.

The understanding of a coating's life cycle helps in streamlined, objective research and development, targeted application, effective and efficient manufacturing, and maintained process/product quality. The life cycle consists of research and development, application, manufacturing, and quality control, shown in Figure 1. The steps in life cycle phases support identifying technology, defining and prioritizing customer needs, translating them into critical part/assembly characteristics/target values, developing production equipment requirements, and establishing process control methods/parameters and inspection routine. The importance of standardized coatings testing, preparation, evaluation, and characterization technique is underestimated in some sectors, which has led to passing of a non-optimal coating and failing of a good one. Either scenario is unacceptable.

There are four main categories of coatings applied in gas turbines: thermal spray, overlay, diffusion, and environmental barrier coatings (EBC).

Thermal spray coatings are widely used in aerospace, nuclear, power generation, transportation, pulp and paper, petrochemical, oil and gas, medical, and automotive industries. Some of their applications are clearance control, thermal barrier, corrosion protection, wear resistance, decoration, dimensional restoration, etc. Thermal spray is a board term that encompasses many spray techniques based on energy source, particle velocity, state of feedstock, and spray mode.

Overlay coatings are applied onto a surface in a vacuum chamber or reactor. Feedstock of the coatings are wire, powder, rod, bulk material, and precursor gases.

Diffusion coatings are applied in a vacuum as well, but the thermodynamic equilibrium of the coatings-substrate materials shift resulting in adsorption of coatings material leading to diffusion of constituent elements from coating to substrate or substrate to coating.

EBC is applied onto a surface via thermal spray, air spray, as slurry, and in a chamber-like overlay coating. They are applied on metal substrates, ceramic matrix composites, and continuous fiber-reinforced

Figure 1: Life cycle of coatings.

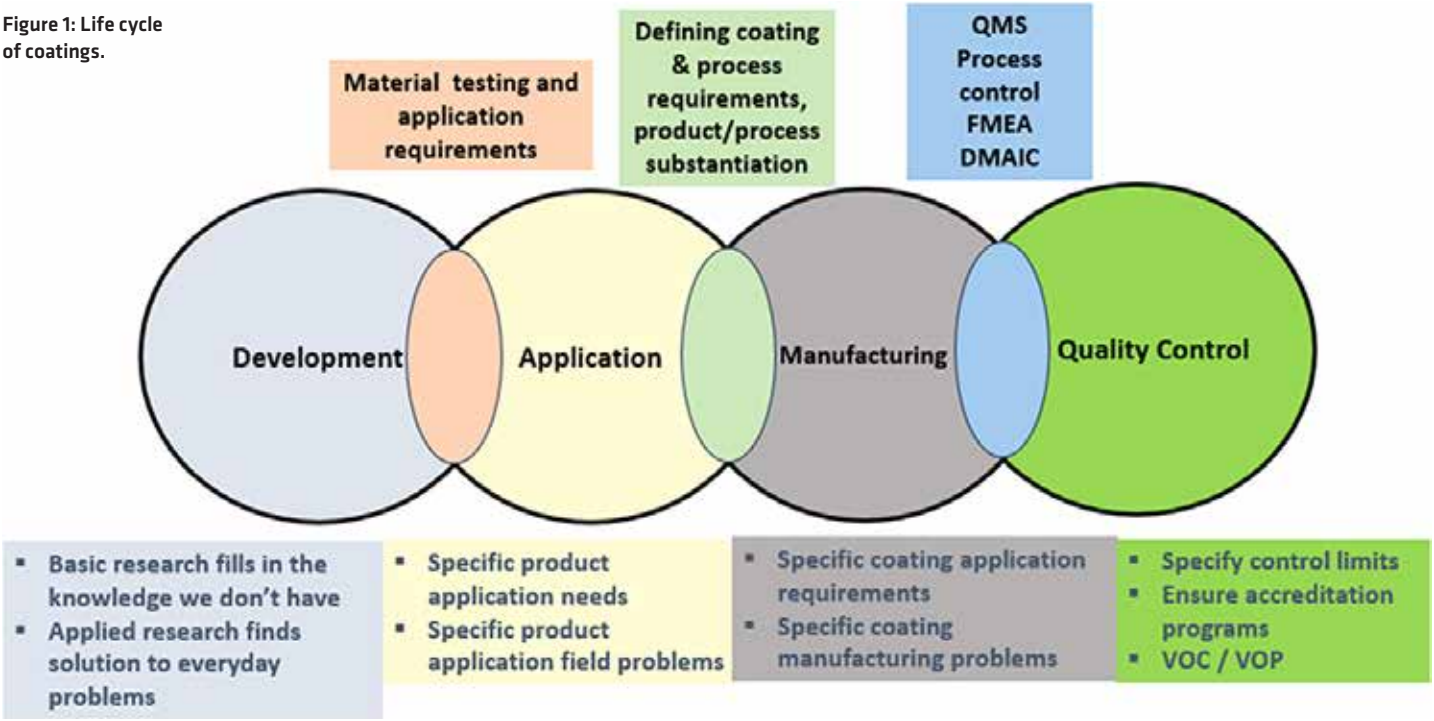

ceramic composite combustor liners. These coatings protect substrates from high temperature oxidation up to 1,482°C (2,700°F), corrosion, wear, and water vapor recession.

A variety of methods used to apply these coatings is considered a special process in many industries, thus it must be substantiated before deployment and controlled afterwards. The life-cycle phases of these coatings are critical in ensuring that a knowledge base exists for understanding process and materials behavior, correct technology is chosen for a product/specific problem, process and coating requirements are established, and repeatability and reproducibility of the process is guaranteed.

Duration of a technology from inception to maturity to production can take five to 10 years. Coatings research and development consists of creation and development of new coating materials, creation and development of methods and processes for application, and understanding the interaction between coating systems and coating methods. It focuses on basic research to fill the knowledge we don't have with the objective of solving everyday problems.

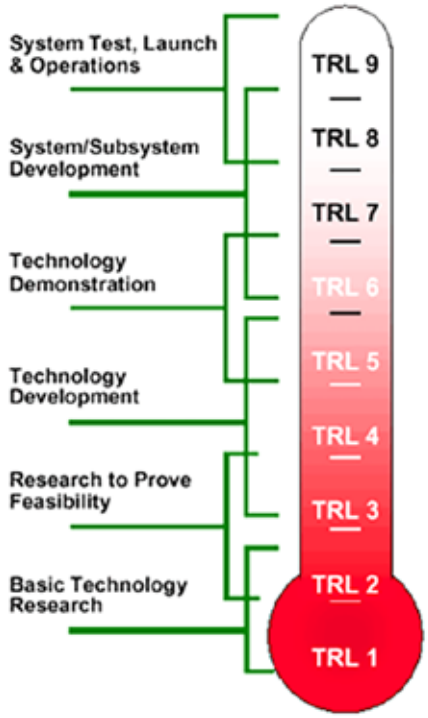

Figure 2: Technology readiness level.

A structured technology readiness level (TRL), shown in Figure 2, and manufacturing readiness level programs that move through rigid tollgate phases are a necessity for technical competency, timely validation, and cost effectiveness. The TRL 1 indicates the beginning of research. Findings and understandings from preceding levels set the objectives of successive levels. Materials testing and evaluation play a vital role in understanding the materials science paradigm of processing, structure, property, performance, and characterization, which supports product validation. Some of the testing applicable to coatings are metallographic, bond strength — tensile and lap shear, hardness, erosion, oxidation, composition, wear, fatigue, corrosion — wet/environmental, and residual stress. At TRL 8, the technology is "flight ready" for application.

The application phase is focused on selecting a coating and method for a specific application on a product/part. A coated part used in gas turbines is shown in Figure 3. The selection of coating material and coating method are dependent on compatibility of the method on hardware, materials degradation issue that is being addressed, reproducibility, manufacturability, repairability of the coatings, cost, and field application. Leading a transition from R&D to product qualification/certification needs a disciplined approach. Part application development is run through a series of tollgates. The initial tollgate is to select a critical but low risk part, review equipment, funding levels, resources, and project timeline. A spray, test, repair, and part substantiation plan needs to be established before developing specifications and validation test and analysis. If there are any disconnects between controlled environment and field application, specifications need to address those concerns. Upon successful completion of application development, we are ready for the manufacturing phase.

At this stage, the R&D and application team hands over projects to the manufacturing team. The manufacturing phase is driven by coating and application requirements. A typical coatings manufacturing process map is shown in Figure 4. A detailed value stream mapping will help a team in understanding the cycle time, changeover time, and takt time. The team should follow lean manufacturing methodology to minimize waste and drive efficiency. Lean methodology sees nine forms of waste with the acronym DOWNTIMES. D – defect; O – overproduction; W – waiting; N – non-utilized talent; T – transportation; I – inventory; M – motion; E – extra processing; and S – safety. To drive manufacturing excellence, manufacturing teams ought to minimize DOWNTIMES. Furthermore, going to Gemba, Kaizen, waste walk, 6S, Kanban, Poka-Yoke, and Cellular manufacturing principles in combination with Six Sigma methodology is deployed for optimal quality management system.

The quality control phase works in tandem with the manufacturing phase. Manufacturing processes need to be controlled and continuously managed to ensure that the process has not drifted. Six Sigma

Figure 3: A coated high-pressure internally cooled turbine nozzle guide vane. [1]

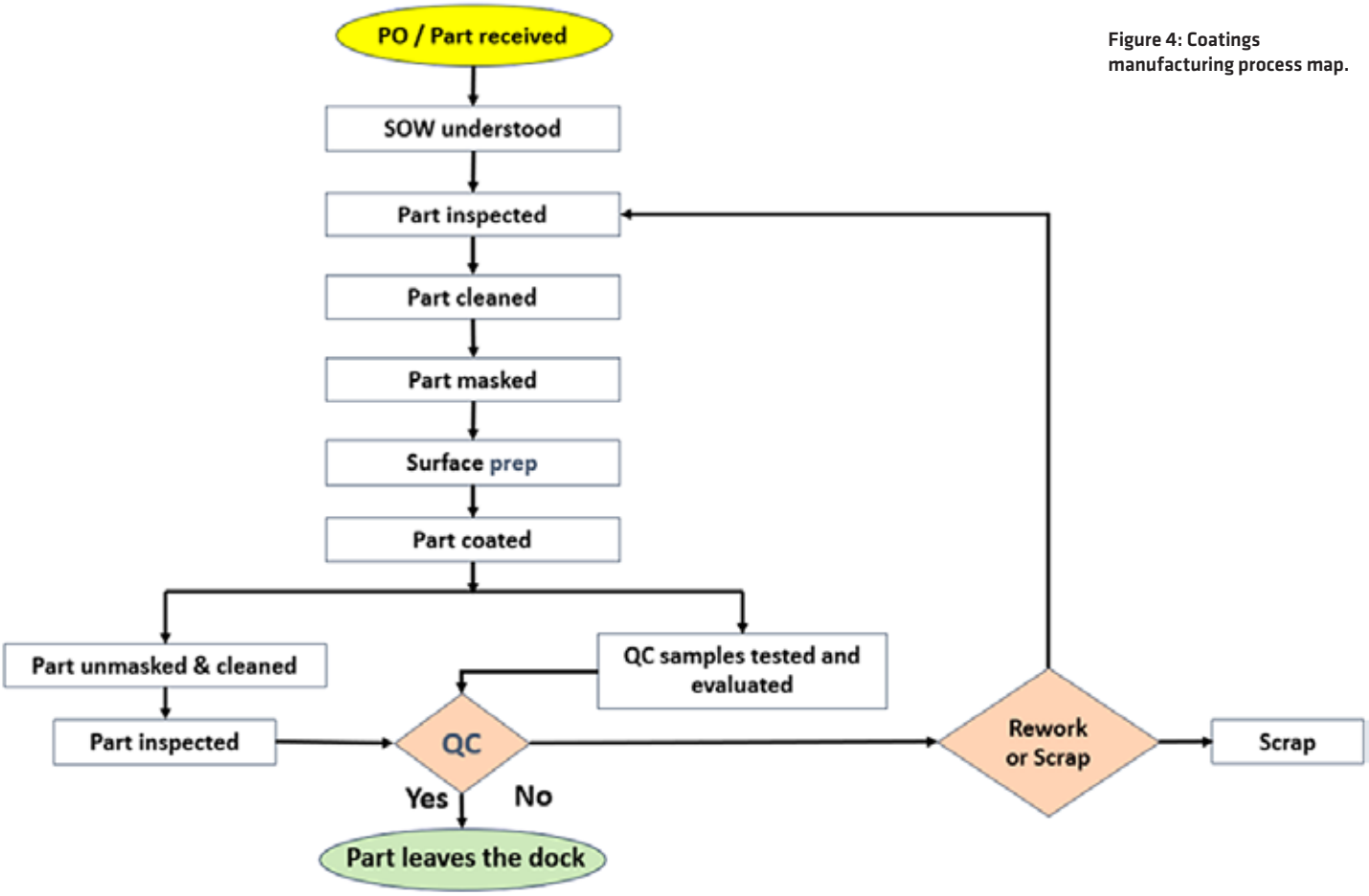

Figure 4: Coatings manufacturing process map.

methodology will ensure effectiveness of the program. Failure Mode and Effect Analysis (FMEA), a risk management tool, is used to identify potential failure, anticipate consequence of failures, and mitigation. The severity of failure, frequency of occurrence, and detection ability must be understood to compute a risk priority number for effective corrective action. In coatings, the failure will arise from the coating method, surface preparation, coating performance, and the part. Statistical process control charts, such as individual range, moving range, subgroup average, and range of subgroup is applied to monitor a process and to improve it through elimination of assignable causes and reduction of process variability. Sigma level of current process is calculated, and a target sigma level is established based on Defects per Million Opportunity. Process capability indices, such as Cp and Cpk and Pp and Ppk measure short-term and long-term process stability, respectively. It also gives insight into how the process variation — voice of process (VOP) compares to the targeted specification/engineering variation — voice of the customer (VOC). Process capability is measured for coatings characteristics, such as porosity, unmelts per field of view, elemental composition, transverse crack per linear inch, oxides, thickness, grit embedment, bond strength, hardness, surface roughness — pre-coating and post-coating, extent of oxidation, erosion, wear, fatigue, etc. A Pareto chart must be constructed to identify the biggest contributors to problem(s). The contributors can be any one of the 6Ms: Man, Machine, Material, Method, Measurement, and Mother Nature. To confidently evaluate the extent of which contributor is causing the observed problem, Design of Experiment (DoE) is exercised by making purposeful, systematic changes. DoE can be deployed in all phases of the life cycle. We need to be careful that correlation does not mean causation. It is convenient to conclude that the effect of input variables is direct. Unfortunately, that is not the case for complex processes such as a coating's application, testing, and evaluation. The effect can be due to the interaction of input variables. A full factorial DoE with resolution V designs can help identify that. Further, Analysis of Variance helps in understanding the significance of individual variable and interaction of variables at appropriate alpha levels.

The Define, Measure, Analyze, Improve, and Control (DMAIC) steps can be applied in all four phases in various forms to achieve targeted objectives. As the complexity of coating material, coating process, hardware, and environment increased, the DMAIC cycle has been modified to Define, Measure, Analyze, Design, and Verify the cycle as a part of the Design for Six Sigma practice. The Design for Six Sigma practice is being used for design/development, innovation, optimization, and validation of product/process to achieve effectiveness. The methodologies, principles, and techniques presented here are applicable and can be employed in many other industries, such as heat treatment, materials processing, etc.

REFERENCE

[1] Olivier Cleynen, CC BY-SA 3.0 <https://creativecommons.org/licenses/by-sa/3.0>, via Wikimedia Commons

ABOUT THE AUTHOR

Triratna Shrestha is the manager of Material Analysis Laboratory and Central Coatings Laboratory at Metcut Research Inc. He has worked with coatings for aerospace, petrochemical, and power-generation applications and has expertise in materials testing and evaluation. He manages Central Coatings Laboratory for GE Aerospace and is involved in failure analysis and in implementation of Lean Six Sigma methodologies. He received his B.S and Ph.D. in Materials Science and Engineering from the University of Idaho. He can be reached at tshrestha@metcut.com.

YOUR RESOURCE FOR HEAT TREATING SERVICES

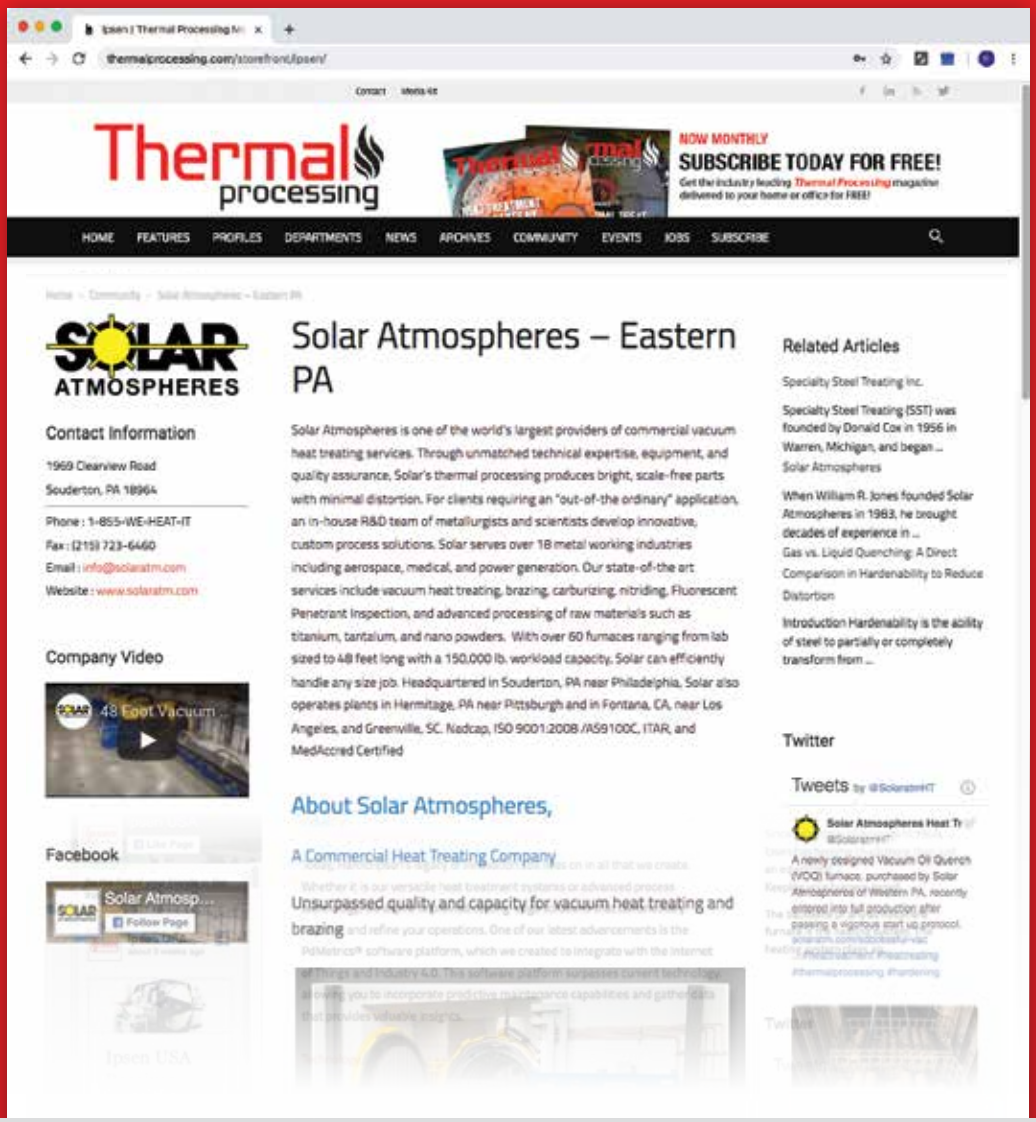

The Thermal Processing Community is your online source for commercial heat treaters, equipment, testing and services.

Search our community for heat treaters by state or services, where you'll find company profiles and contact information.

Our listings are organized so you can easily find companies that meet your heat treating needs.

Find this and more at ThermalProcessing.com.

Not listed in our community storefront? For information on how your company can join and reach more customers, contact

Susan Heinauer – regional sales manager
412.897.0287
susan@thermalprocessing.com

Thermal processing

D. SCOTT MACKENZIE, PH.D., FASM
SENIOR RESEARCH SCIENTIST–METALLURGY /// QUAKER HOUGHTON INC.

Creep is a process of applied stress at elevated temperatures greater than 40-50 percent of the absolute melting temperature, resulting in plastic deformation of the part.

The mechanism of creep and its stages

In this column, I will discuss the mechanism of creep and its three stages.

Applications of metals at elevated temperatures involve several problems. It is known that the strength of metals decreases as the temperature increases. As temperature increases, the rate of diffusion increases. The equilibrium concentration of vacancies also increases as temperature increases. Dislocations have increased mobility at elevated temperatures through the mechanism of climb. The slip system of a metal may change as the temperature increases. The microstructural stability of the material is also of concern, as cold worked metals may recrystallize and exhibit grain coarsening. Precipitation hardening alloys, such as aluminum, may overage and lose strength as the precipitates coarsen.

Creep is the time-dependent plastic deformation of a metal or material under load. Creep usually occurs at high temperatures but can also occur at room temperature. Good examples are lead or glass. The concept of high temperature varies from material to material, as one temperature is high for one material, but not high for another material. In general, creep is considered to occur at 0.4-0.5 T_m, where T_m is the absolute melting temperature of the material (measured in °K).

When measuring the engineering creep curve of a metal, a constant axial load is applied to a tensile specimen maintained at a constant temperature. The elongation of the specimen of the specimen is measured as a function of time. The general procedures of creep testing are described in ASTM E139 [1].

The idealized shape of a creep curve is shown in Figure 1. In this curve, there are three primary stages. Primary creep where there is an initial rapid elongation of the specimen, which then decreases with time. This creep rate eventually reaches a steady state in which the creep rate changes very little with time. This is called secondary creep. In the final stage of creep, called tertiary creep, the creep rate increases rapidly until fracture occurs.

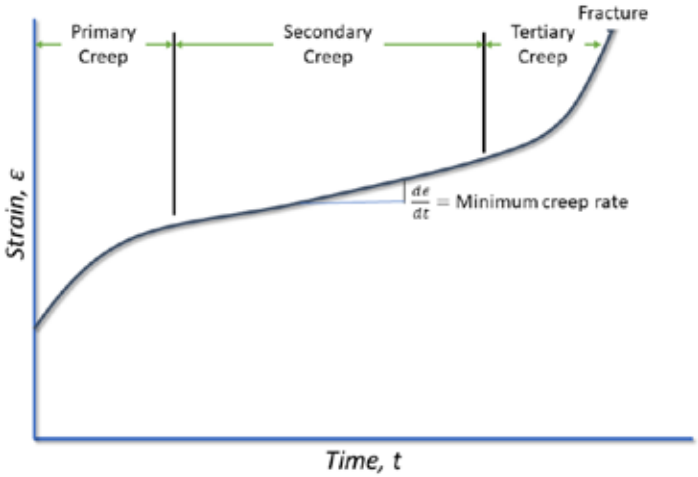

Figure 1: Typical creep curve showing the three stages of creep in a constant load test [2].

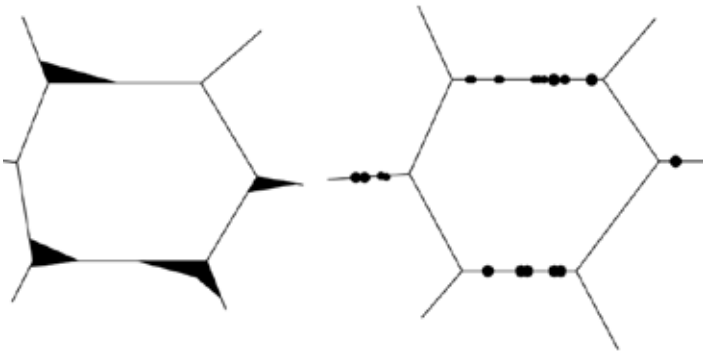

Figure 2: Creep cavities and voids forming along grain boundaries resulting from mass transport.

STAGES OF CREEP

The first stage of creep, called primary creep, represents a region of decreasing creep rate. This is predominantly a transient creep, where the resistance to creep by the material increases due to the deformation of the metal.

The second stage of creep, or secondary creep, is a period of nearly constant creep. This is because of the competing processes of strain hardening and recovery. This steady-state creep is called the minimum creep rate.

Tertiary creep occurs during constant-load testing at high loads and elevated temperatures. This is where there is a reduction in the cross-section of the tensile specimen because of necking (or internal void formation). This stage of creep is often associated with metallurgical changes in the metal, such as precipitation coarsening, or recrystallization.

The minimum creep rate is the most important design parameter from the creep curve. This is typically represented by the stress required to produce a creep rate of 0.001% per hour or 1% in 10,000 hours.

There has been a great deal of research into the mechanisms of creep deformation [3]. The primary dislocation mechanisms are:

- Dislocation glide.
- Dislocation creep.
- Diffusion creep.
- Grain boundary sliding.

Frequently, there will be more than one mechanism occurring at one time.

Dislocation glide involves dislocations moving along slip planes. Any barriers are overcome with thermal activation. This generally

occurs at higher stress levels than would be considered for creep deformation. The creep rate is determined by the ease in which dislocations are impeded by obstacles, such as precipitates, and other dislocations.

Dislocation creep occurs by dislocation glide aided by vacancy diffusion. This is based on the idea that steady state creep is based on the competing mechanisms of strain hardening and recovery by the annihilation of dislocations.

At higher temperatures and lower stresses, diffusion creep becomes the dominant mechanism. Nabarro [4] and Herring [5] proposed that the creep process was controlled by stress-induced diffusion. They suggested that vacancies flowed from grain boundaries with tensile stresses to those that have compressive stresses, while there is a flux of atoms in the opposite direction, elongating the grain. They further suggested an equation where increasing grain size reduced the creep rate.

At lower temperatures, grain boundary diffusion dominates. This is called Coble creep [6]. In this case, Coble creep occurs through the diffusion of atoms along the grain boundary. The activation energies are different for Nabarro-Herring creep and Coble creep. From examination of the activation energies, the dominant mechanism can be determined.

Grain boundary sliding is not a significant contributor to steady-state creep, it is important for initiating intergranular fracture. Since there is mass transport from both Nabarro-Herring creep and Coble creep, voids can form at grain boundaries. Grain boundary sliding is motion of the grain boundaries to accommodate the mass transport from Nabarro-Herring and Coble creep. Voids and cavities can result at these grain boundaries (Figure 2).

Large grains slow this process, as there is less total surface area than with small grains. In a limiting case of single crystals (such as in a jet turbine blade), this mechanism is completely suppressed because there are no grain boundaries.

Precipitates can pin grain boundaries and prevent grain boundary sliding. Fine carbides, or other precipitates, can reduce grain boundary sliding. These precipitates must be small, as large precipitates can initiate voids at the interface, resulting in faster grain boundary sliding.

CONCLUSIONS

In this short article, the mechanisms of creep were briefly described. Creep is a process of applied stress at elevated temperatures greater than 40-50 percent of the absolute melting temperature, resulting in plastic deformation of the part. Large grain size reduces creep and is partially the reason that castings have preferred creep properties over wrought products of the same nominal composition.

Should you have any questions on this article, or suggestions for further articles, please contact the writer or the editor.

REFERENCES

[1] ASTM, "ASTM E139-11(2018) Standard Test Methods for Conducting Creep, Creep-Rupture, and Stress-Rupture Tests of Metallic Materials," American Society for Testing Materials, Conshohocken, PA, 2018.

[2] G. E. Dieter, Mechanical Metallurgy, New York, NY: McGraw-Hill, 1976.

[3] M. E. Kassner and M. T. Perez-Prado, Fundamentals of Creep in Metals and Alloys, New York: Elsevier, 2004.

[4] F. R. Nabarro, Report of a Conference on Strength of Solids, London: Physical Society, 1948, p. 75.

[5] C. Herring, "Diffusional Viscosity of a Polycrystalline Solid," J. Appl. Phys., vol. 21, pp. 437-445, 1950.

[6] R. L. Coble, "A Model for Boundary Diffusion Controlled Creep in Polycrystalline Materials," J. Appl. Phys., vol. 34, pp. 1679-1682, 1963.

ABOUT THE AUTHOR

D. Scott MacKenzie, Ph.D., FASM, is senior research scientist-metallurgy at Quaker Houghton. He is the past president of IFHTSE, and a member of the executive council of IFHTSE. For more information, go to www.quakerhoughton.com.

FINITE ELEMENT MODELING AND SIMULATION OF VACUUM BRAZING PROCESSES

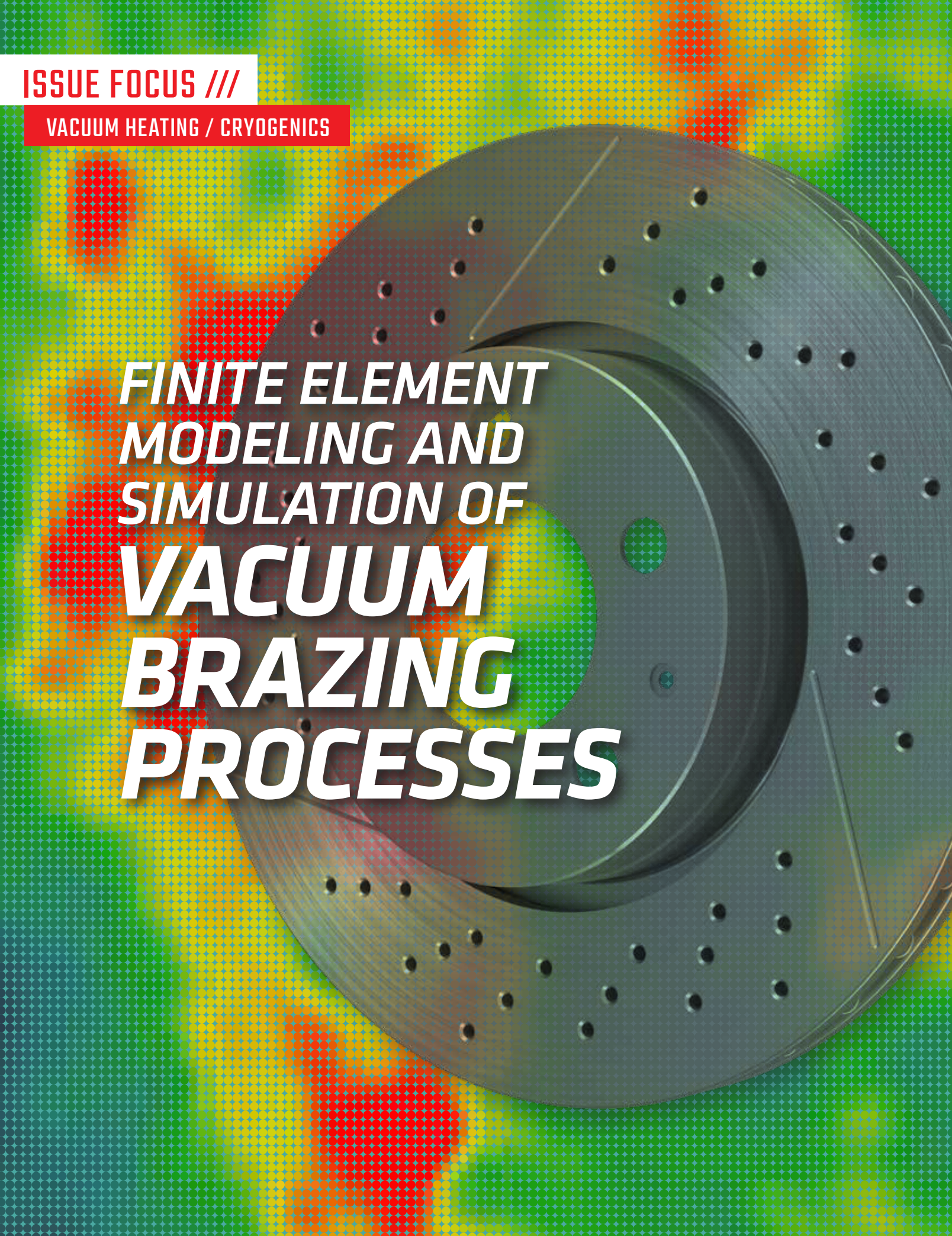

In this study, a new method of radiation and contact modeling was developed to identify the most critical influencing factors of distortion for vacuum brazed assemblies with simulation.

By WOLFGANG TILLMANN, TIM HENNING, LUKAS WOJARSKI, CHRISTIAN TIMMER, and FINN ONTRUP

Vacuum brazing is a black box process, so component distortion that occurs during heat treatment is difficult to prove experimentally. Thus, a novel FE-model was developed in ANSYS Workbench to calculate the time and location resolved component deformation of AISI 316L/B-Ni2 brazing assemblies. In this regard, a new method of radiation and contact modeling was developed that enabled a significant reduction of the calculation times and solved the convergence issue for simulating the distortion of large-scale, thin components. The results showed the component deformation during heating can be easily kept in the elastic range and can be almost completely eliminated by using a geometry-dependent soaking time. In contrast to this, high cooling rates were found to result in thermally induced stresses well above the elastic yield limit, causing significant component deformation. With further cooling, the deformation decreases significantly, but it depends on the initial stress state, the geometry, and the cooling rate whether the deformation can be completely leveled out during the shrinkage of the component. Thus, the initially high cooling rates were identified to be responsible for the final distortion. Furthermore, this was highly affected by the local position in the heating chamber. The simulation results were used to design a fixture for vertical positioning, which reduced the maximum temperature difference in the brazing assembly from 141 to 79°C, the maximum interim distortion from 275 to 31 µm, and the final distortion from 14 to 8 µm.

1 INTRODUCTION

There are mainly two application cases in brazing processes, where distortion is evident to the quality of the brazed part. On the one hand, there are assemblies with thin or greatly varying material thicknesses [1,2,3,4]. In addition to this, different materials are frequently used, so that a significant stress level is induced in the brazed part during cooling due to differing coefficients of thermal expansion [5,6,7,8,9]. Examples of this are cemented carbide/steel- and ceramic/steel-joints, in which cracks occur in the cemented carbide or in the ceramic whenever stress conditions are too high, despite the often small joining surfaces [7, 8, 10,11,12]. In addition to processing strategies, such as the use of brazing foils with a ductile interlayer made of copper, simulation-based optimization of the process is usually applied for this purpose [7, 13,14,15,16,17,18,19,20,21]. On the other hand, there are assemblies with integrated cooling channels at the joint level, primarily in toolmaking, for which distortion leads to leakage and thus to the failure of the component [15, 22]. An example that illustrates these relationships quite well is a brazed component from EUV-lithography, which is important to manufacture latest generation semiconductors and CPU cores in the nm range [23]. A copper mirror is joined to a stainless-steel substrate and features an internal cooling channel structure. The component is used to deflect extreme ultraviolet radiation (EUV) of a high-power laser; therefore, it must meet exceptionally high requirements for geometric precision as well as being continuously cooled. Another example is characterized by injection molds, which often have cooling channels integrated at the joint level to enable conformal cooling during injection molding [15].

All these examples illustrate the extraordinarily high demands on the control of component distortion in vacuum brazing processes, which require a lot of experience. Further challenges result from a wide range of influencing variables for distortion and large industrial batches of different components and, in particular, because component distortion cannot be easily determined during the process [24, 25]. From a brazing point of view, component deformation primarily leads to a widening of the joint gap, so that a depletion of the applied filler metal occurs and results in the formation of large cavities in the joint. In the case of the frequently used nickel-based brazing filler metals, the widening results additionally in the formation of continuously pronounced intermetallic phase bands that dramatically impair the joint strength [26,27,28]. In general, such phase bands cannot be avoided in brazing processes of common steels above a gap width of about 50-70 µm while complying with the heat-treatment specifications. Furthermore, the conditions of the components supplied by the user are often unknown with regard to the pretreatment (e.g., cold-, hot-, or cross-rolled, plane grinded, face milled) and the resulting residual stress state for the heat-treatment operation. For financial reasons or material technology (e.g., AISI 316L), not every component can be annealed in a stress-relieved way before joining. Therefore, the residual stress state is expected to be one of the most important influencing variables to be considered in the design of the heat-treatment process. Anyway, the main procedure to control component distortion in practice is characterized by defense heating and cooling rates, which increases the manufacturing time and therefore the costs significantly. The design of the associated temperature-time cycles is usually experience-based and offers a high potential for improvement if the process segments causing distortion can be identified simulatively [29, 30].

The simulation of vacuum brazing processes for specific component geometries is an adequate method to assist the brazer in the design of the temperature-time cycle, the adjustment of the batch size, and the local positioning of individual parts [25, 31, 32]. A particularly valuable advantage of the simulation is the possibility to advise and support the customer already in the design phase of the component with regard to heat-treatment distortion. In this context, a simulation tool is needed that allows moderate calculation times and is, therefore, likely to be subject to some restrictions in terms of accuracy. Nevertheless, such a simulation makes it possible to identify distortion-critical process segments and to evaluate a suitable component position. It also provides an important basis for deriving improvements such as additional loading by weights or the design of a fixture to braze the component with a minimum of distortion.

From a research point of view, the finally developed simulation tool will be used to investigate the extent to which full- or partial-surface additional bodies influence the resulting component distortion. The additional bodies are expected to significantly affect the heating and cooling behavior by selectively increasing or decreasing thermal gradients within the component. They, therefore, reduce thermally induced stresses that lead to distortion. For the material selection of these additional bodies, primarily the heat capacity and the thermal conductivity are of interest, while the geometric shape can be freely designed. Before these interdependencies can be investigated, it is necessary to develop the simulation model itself. An initial starting point of the project is based on investigations by Tennenhouse, who stated that the allowed temperature difference ΔT to keep the material distortion within the elastic limit can be calculated by Equations 1-4 where ε is the strain, C the thermal coefficient of expansion, S_y the yield strength, and E the modulus of elasticity [33].

$$\epsilon = C\Delta T \quad \text{Equation 1}$$

$$\epsilon = \frac{S_y}{E} \quad \text{Equation 2}$$

$$Substitution : C\Delta T = \frac{S_y}{E} \quad \text{Equation 3}$$

$$Solution : \Delta T = \frac{S_y}{EC} \quad \text{Equation 4}$$

Based on the mostly known temperature-dependent values of the thermal coefficient of expansion and the modulus of elasticity, an acceptable temperature difference within the component results for each process temperature. That way, the elastic deformation is completely eliminated at the end of the process at zero-temperature difference. At the time this relationship was evaluated in 1971, graphs were derived from these equations manually to design distortion-minimized temperature-time cycles with respect to the material used. Today, this procedure is automatically integrated by the definition of the materials data and multilinear plasticity hardening model in simulation. Determining the values for the plasticity behavior at high temperatures presents a particular challenge, because the yield point, which represents the elastic limit, can generally no longer be determined exactly [34,35,36]. However, it is precisely this material data set that is critical for an accurate prediction of component distortion. Therefore, the definition of the material data is particularly vital.

In this article, the goal is initially given by a new development of an FE-model and the fulfillment of basic requirements to simulate vacuum brazing processes. A key requirement is characterized by a free positioning of one or several brazing assemblies. Therefore, it is not possible to simplify the model using symmetry planes or to use symmetry surfaces as a definition for supports which makes it very challenging to achieve a convergent solution for large brazing assemblies. The novelty of the model is based on a simplified radiation modeling, which enables the usability of real vacuum furnace temperature data as an input variable. Furthermore, a new method of contact modeling will be investigated to enable the free positioning of the components, and thus, the distortion of the brazing assemblies can be analyzed for individual temperature–time cycles and positions within the heating chamber.

2 MATERIALS AND METHODS

In this section, the materials and methods used for the experimental brazements as well as simulations are described in detail.

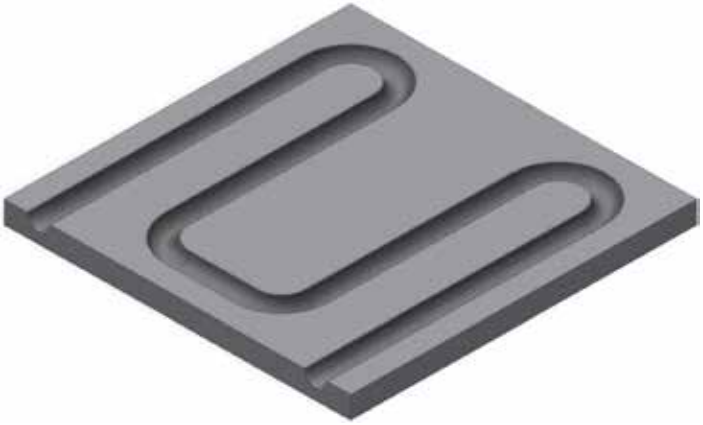

Figure 1: Geometry B 150 × 150 × 10 mm with a milled cooling channel at the joint level (AISI 316L).

Geometry & ID	Alignment	Orientation	Heating rate [°C/min.]	Soak level at 900 °C, 10 min.	Max. process temperature [°C]	Dwell time [min.]	Cooling mode
A1	0°	centered	15	Yes	1060	25	VC
A2		lateral	50	–	1110	5	N_2
A3	90°	centered	50	–	1110	5	N_2
A4		lateral	15	Yes	1060	25	VC
B1	0°	centered	50	–	1110	5	N_2
B2		lateral	15	Yes	1060	25	VC
B3	90°	centered	15	Yes	1060	25	VC
B4		lateral	50	–	1110	5	N_2
A5	0°	lateral	25	Yes	1060	10	VC
A6	90°	centered					N_2
B5	0°	centered					VC
B6	90°	lateral					N_2

Table 1: Experimental design with varied parameters.

2.1 Manufacturing process of samples and their geometry

AISI 316L austenitic stainless steel was selected in order to build up the FE-model without an additional microstructural transformation effect. Two different geometries were defined to investigate the two main application cases mentioned in Section 1. For geometry A, a 5-mm-thick hot-rolled plate of size 200×100 mm will be joined on top of a just 2-mm cold-rolled plate of the same dimension. Because of the requirement to produce a sufficiently large distortion for building up the FE-model, different rolling conditions need to be used. Moreover, hot-rolling processes are typically not applicable to thin sheet metals. The different material thicknesses and the normally unfavorable length-to-width ratio of 2:1 were also specified in order to be able to investigate the effects within the experimental design on the resulting component distortion with certainty. Figure 1 illustrates geometry B for which two hot-rolled sheets of thickness 10 mm and dimension of 150×150 mm were brazed together to create an integrated cooling channel of diameter 10 mm. The minimum distance between the milled-in cooling channel and the rim of the component is 10 mm, which ensures a leak-tight connection with regular brazing processes.

The samples were cut from the strip by waterjet cutting, and then

straightened with roll precision to finally be machine-grinded with a grit size of K240 to an evenness below±10 µm by Kaiser Präzision GmbH. AMS 4777 (B-Ni2) nickel-based brazing foil with the thickness of 50.8 µm was used from the Prinze&Izant Company for the experimental brazing processes. The amorphous brazing alloy contains mainly 7.0% Cr, 4.5% Si, 3.125% B, and 3.0% Fe with silicon and boron serving primarily as melting point depressants, which enables a melting range of 971-998°C.

2.2 Experimental design

Table 1 illustrates the experimental design that was used to evaluate significant influencing variables on component distortion for geometries A and B. The varied parameters are characterized by the local position in the heating chamber, the temperature-time cycle, and the cooling mode. It should be noted the respective parameters were performed both experimentally and in simulation so the results can be compared in order to adapt the simulation more to reality.

The alignment of brazing assemblies with geometry A is defined as 0° when the longer edge is aligned in the longitudinal direction of the rectangular heating chamber and 90° when the positioning is transverse to it. In the case of square geometry B, the degree represents the orientation of the cooling channel. In addition to this, a lateral orientation designates a local position on the edge of the usable area of the furnace with the smallest possible distance to the heating elements. The heating rates of 15 and 50°C/min were again explicitly chosen higher than usual in order to generate sufficient distortion if this should be characteristic for the respective process segment. Furthermore, the extent to which a soak level (900°C, 10 minutes) affects the stress state of the brazed components was investigated. In addition, the maximum process temperature and the dwell time were varied. Out of the 12 test series shown in Table 1, an additional simulation was carried out for the last four below the line, which was primarily intended to significantly reduce the calculation time.

With regard to the resulting distortion, the temperature is evident because higher temperatures result in higher temperature gradients between the edge and the core of the brazing assembly during cooling. The dwell time probably determines the stress relief, which serves as the initial state for cooling and is then superimposed with the cooling stresses. It is expected that the greatest stresses will occur during the cooling phase, so two different methods were investigated. With vacuum cooling (VC), the heating is switched off, and the batch cools down by thermal radiation losses quite quickly at first and very slowly at very small temperature differences. This is due to the Stefan-Boltzmann equation in which the temperature enters with the fourth power for the emitted radiation. At low temperatures, the radiation losses are quite small and it is time-consuming to cool down the batch completely in vacuum. Overpressure gas cooling with inert gas (e.g., N_2) is frequently used for such brazed components to enhance the economic efficiency or beyond that to harden martensitic hardenable steels. In the case of AISI 316L, an overpressure gas cooling is mainly used to avoid a formation of the σ-phase, which affects the corrosion resistance [37,38,39,40,41].

2.3 Stress relief annealing and evaluation of temperature distributions

Prior to conducting the experimental design, a preliminary study was conducted on the effect of stress relief annealing on the resulting component distortion. Stress relief annealing is not recommended for AISI 316L, as it affects corrosion resistance. Nevertheless, a preliminary study was carried out in order to transfer the results to other steels and to evaluate the extent to which stress relief annealing already produces component distortion. For this purpose, three samples each of geometries A with a thickness of 2 and 5 mm and geometry B were annealed at 650°C for 2 hours in the vacuum furnace, which is described in the next subsection. A heating rate of 10°C/min and vacuum cooling were used. Afterwards, the distortion of these samples was compared to the as-delivered condition using a 3D scanning method which is described in Section 2.5. Furthermore, the biaxial residual stress state of the surface was determined for all these samples by X-ray diffraction using a Bruker D8 Advance device. Peak (311) was chosen for the determination of residual stresses because it is at high 2 Θ angles and has a narrow peak width. Furthermore, this peak showed a significant lower texturization than peak (200). Thus, the measurements were conducted at 40 kV and 40 mA with Co-K_α radiation for 2 Θ angles between 108 and 114°, using a step size of 0.1° and a time-per-step of 1 second. Φ was set to the range of 0-45° and Φ to the range of 0-270° with several equidistant intermediate steps.

2.4 Heat treatment and brazing

All heat treatments and brazements were carried out using a vacuum furnace of type EU80/1H 2RV from IVA Schmetz GmbH. The heating chamber is rectangular with an inner size of 660 × 430 × 460 mm (l × w × h). The heating elements are made of twisted wires of molybdenum and laid in a meandering pattern in the vicinity of the internal surfaces of the chamber with the exception of the front door and the back. The internal surfaces are made of several thin molybdenum sheets with some space in between, so that a heat distribution within the heating chamber of $\Delta T \leq 2°C$ can be assured for the usable area of the furnace. The outer surfaces of the heating chamber are made of a stainless-steel weld construction, inserted in a double-sided and water-cooled enclosure. Six load supports of Ø16 mm and a length of 230 mm protrude from the bottom of the tubular enclosure into the interior of the heating chamber and are isolated by Al_2O_3 tubes (Ø22 mm, h=100 mm, t=2 mm) on the inside. On top of these supports, three elongated U-profiles of molybdenum are placed, with a size of 550 × 24 × 3 mm each (l × w × t), on which the batch is finally placed on the top of a molybdenum sheet of the size 300 × 274 × 4 mm (l × w × t). The allowed usable area is of the size 350 × 250 mm and is between the centers of the outer U-profiles with regard to the longitudinal axis.

For the control of the max. 80 kW heating capacity, a sheath thermocouple type C (Ø3.2 mm W5Re-W26Re) near the heating wires is used as an actuating variable within the PID-control loop. In addition, six thermocouples type N (Ø1.5 mm NiCrSi-NiSi) can be used to measure the temperature of the batch. Prior to the heat treatments and brazements, the measuring section was calibrated using a loop calibrator of the type DPI 812 device of GE Inc. Subsequently, the six batch elements were inserted 5 mm deep into drill holes of a test sample. The calibration was checked with an experimental furnace run at several temperature levels, which revealed a maximum $\Delta T \leq 2°C$. To perform the brazements later on, furnace runs with dummy specimens of geometries A and B were first performed with the individual temperature-time cycles and the local position of the brazing assemblies with respect to Table 1. Thereby, three thermocouples were placed into the upper part and three into the lower part of the brazing assembly at the center, the edge, and the center of the longitudinal edge. This is necessary because program control according to the batch temperature leads to different process times depending on the positioning of the components. Afterwards, the brazements were conducted based on these individual temperature-time cycles and controlled only by the heater thermocouple. This way, the brazing assemblies were not affected by the drill holes for the batch thermocouples.

2.5 Optical 3D measurement of distortion

The measurements for the distortion of the components were carried out on the top side of the heat-treated samples and the brazed components with the optical 3D measuring system ATOS II Triple Scan from Carl Zeiss GOM Metrology GmbH (accuracy 20–62 µm). Several measuring marks were stuck on the top surface. Then, AESUB-Blue-Scanning spray was thinly coated on top of the component's surface and the edges. Afterwards, the component was placed on a rotating plate with additional measuring marks. Within the scope of the measurement, seven individual measurements were taken from each of two different angles. As a result, a polygon-shaped surface can be calculated from the single measuring points. This surface was superimposed using a 3-2-1 best-fit-method to an ideal even surface of the same dimension. It was constructed by CAD in GOM Inspect software. This allows the deviation of the two surfaces to be determined (distortion), visually displayed with false colors, and locally evaluated numerically. It is generally more useful to scan the component before and after heat treatment and to compare the respective measurement data directly with each other. Due to the significantly lower measurement effort and a basically identical pretreatment of the components by surface grinding, a super-imposement by CAD ideal bodies was selected. The measuring time can be estimated at merely 2 minutes, while about 15 minutes per component were needed for the data processing.

2.6 Sample preparation for metallographic investigations

Following up on the brazements and the 3D scan of the upper surface for the judgment of the component distortion, an ultrasonic C-Scan was carried out in water on a LS-100 machine from Inspection research & Technologies Ltd. An amplification of 34.4 dB and a scan speed of 10 mm/s was used with a V317 immersion transducer of Olympus Europe SE & Co. KG running at 20 MHz. Based on the C-Scan, characteristic positions for the preparation of metallographic cross sections were determined. Five segments were cut out for each brazed component using a Mecatome T330 cutting machine along with the joint at each outer edge and for the center of the component. Afterwards, these samples were embedded in epoxy resin, grinded, and finally polished with a diamond suspension of 1 µm to reveal the microstructure of the joint. The samples were then cleaned in an ultrasonic bath using ethanol and dried with warm air.

2.7 Development of an FE-model for vacuum brazing

This section exclusively describes the final developed model and additionally explains the most important aspects to be considered when thermal radiation is investigated in brazing simulations. The FE-model was created with ANSYS Workbench 2020 R1 and calculated by an Intel i5-8400 CPU running at 2.8 GHz as well as 128 GB random-access memory. The FE-model allows to consider real heating and cooling rates of a vacuum batch furnace and enables a free shape as well as a free alignment of the components within the heating chamber. The brazing processes were simulated and analyzed individually by a thermal-transient and a structural-transient analysis. For this purpose, the vacuum furnace described in Section 2.4 was used as the basis for building a completely new FE-model. The following describes the development of the model in detail.

2.7.1 Simplifications

With respect to the calculation times, some simplifications were made for the model. Previous simulation results prove it is not necessary to include the water-cooled enclosure in the model. It is sufficient to set a time-dependent temperature specification on the bottom side of the cylindrical load supports. In addition, instead of modeling the geometrically complex molybdenum wire heater, the entire inner surface of the heating chamber can be defined as heating surfaces. The material properties of the brazing alloy AMS 4777 were specified in the technical data by those of pure nickel, since no sufficient data exist for the brazing alloy. The brazing alloy remains in the solid state in the simulations performed, so there will be a change in the contact condition prior to the cooling segment. This implies the model cannot initially be used to investigate the widening of the brazing gap, which was derived from the deformation of the component surface instead. For simulations with overpressure gas cooling, a temperature-dependent heat-transfer coefficient is specified instead of a computational fluid dynamic simulation (CFD). The heat transfer coefficient α was deviated from technical literature with respect to the pressure and the estimated flow velocity [42]. Only two of the three possible U-profiles were used in both the experimental and simulation, so the influence of the local position can be investigated first in this study.

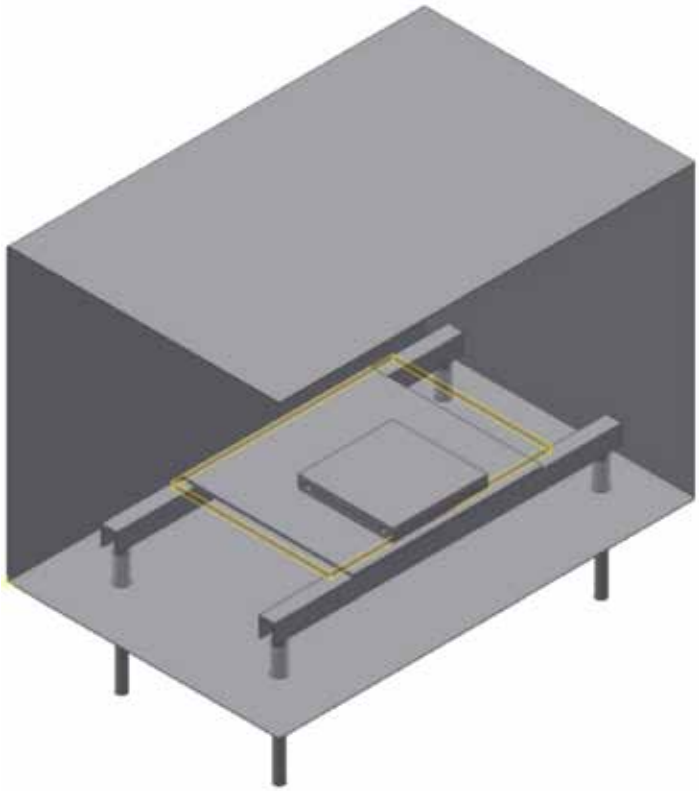

Figure 2: Simplified CAD-Model of the heating chamber with a lateral orientated brazing assembly of geometry B at 0°. The frame shows the limits of the usable area.

2.7.2 CAD modeling of a vacuum furnace

The individual parts of the FE-model were constructed according to the real dimensions of the heating chamber of the furnace described in Section 2.4 using the CAD-software Inventor professional 2019 from Autodesk GmbH. In Figure 2, the CAD-Model is shown with the front and one side of the heater surfaces blanked out for reasons of presentation.

There are some important aspects to consider when assembling the single parts, if thermal conduction and thermal radiation are involved in the simulation. The most important one is the batch and its support are geometrically decoupled from the heating surfaces. This ensures the heat from the heating surfaces is introduced into the batch primarily by thermal radiation and not by thermal conduction. As a result, a small error in the calculation of the view factors in the perfect enclosure type, which was applied later in the simulation, is

present. It is still minimized by the insulating Al_2O_3 tubes and can be considered as negligible. In addition, the designer must consider those surfaces or parts of surfaces that are subjected to thermal radiation can be selected individually. The best way to achieve this is given by the Design Modeler CAD-software included in ANSYS Workbench, in which the surface separation tool can be applied. The six faces of the rectangular heating chamber are connected to each other by the inner corners and inner edges. This offers the advantage that the non-heated surfaces of the front and rear sides are in contact only at one node or node line in the FE-model, thus reducing the influence of heat conduction.

2.7.3 Technical data and meshing

The second step after the construction of the CAD-model is to set the technical data of the materials used in ANSYS Workbench. To calculate the temperature distribution in thermal-transient analysis, the density, the thermal conductivity, the specific heat capacity, and the emissivity of the respective materials are required. For the subsequent calculation of the deformation in the structural-transient analysis, the coefficient of thermal expansion, the Young's modulus, the Poisson's ratio, the strain at failure, and the tangent modulus are necessary. Most of the required material data sets are documented in the ANSYS Granta Selector software as well as in additional technical literature and were imported to ANSYS Workbench. In some cases, the data sets were extrapolated to ensure this spanned the entire temperature range to be investigated within this study. However, a particular challenge exists for the yield strength of the material AISI 316L, which can only be found in the literature up to 870°C and cannot be clearly determined experimentally. Above this temperature, the yield strength was estimated by a factor of 0.35 for the tensile strength, which is significantly reduced in the temperature range of 870-1,100°C from 183 to 23 MPa [34, 35]. Because of these very low strength values and the fuzzy definition between the elastic and plastic material behavior, a precise calculation of the deformation behavior is an extremely challenging task.

If possible, the meshing was performed by the sweep method, using the following element sizes: heating surfaces, 50 mm; load supports, 8 mm; U-profiles and support plate, 10 mm; AISI 316L geometry A, 1.5 mm; AISI 316L geometry B, 5 mm; and brazing filler metal, 1.5 mm. A very coarse meshing was chosen for the heating surfaces since a temperature specification is made for them in the simulation. In contrast, all contact surfaces and the surfaces of the joint were meshed relatively finely. In order to be able to simulate bending and thus the deformation of the component, two divisions in the material thickness were used for the components of the brazing assembly.

2.7.4 Conditions of contacts and definition of load steps

Almost all contacts were defined as symmetric and frictional using a friction coefficient of 0.15 as well the Augmented-Lagrange method using the adapt to touch option for the initial contact elevation. For the joining surfaces, an additional contact was created as a bond. Furthermore, within the structural-transient analyses, a contact type of no separation was used in the heating phase for the contacts of the brazing assembly. It is highly recommended to check the initial contact finding status with the contact tool to proof the accuracy of the imported CAD-data. The load steps were defined in the settings of analysis for the thermal-transient and structural-transient analysis identically. Three load steps were defined, with the first load step mapping the heating segment and calculated with a step size of 60 seconds. The second load step represents the first part of the cooling phase, in which very high rates of cooling are present, so that this step was calculated with a step size of 10 seconds. The third part has comparatively low rates of cooling and was calculated with a step size of 60 seconds. In detail, the third load step was set to begin at 400°C of the heater temperature for processes with vacuum cooling and at 100°C for processes with overpressure gas cooling. Contact step control was added to the structural tree of both analyses for each of the joint surfaces, so at the beginning of the cooling phase, the frictional or no separation contact was deactivated and the bonded contact activated.

2.7.5 Definition of thermal radiation and convection

Based on the brazing processes actually carried out, the temperature of the heater thermocouple was used as the temperature specification for the four heating surfaces in the simulation by using a surface-to-surface type of radiation in a perfect enclosure. An emissivity of one since the reflective part of thermal radiation is already considered by using real process data. In contrast to this, all other surfaces, which are no contact surfaces, were defined using a temperature-dependent emissivity of the individual material. The outer surfaces of the heating chamber were set as perfectly insulated, while the part of the load supports outside radiates to the ambient temperature. For processes with overpressure, gas cooling convection was defined in addition using 5.0^{-5} W/mm^2 °C as heat transfer coefficient.

2.7.6 Structural-transient analysis on thermal-transient results

It was very beneficial to duplicate the calculated thermal-transient project and to then set a structural-transient analysis for the first three entries. After that, the solution of the first thermal-transient analysis can be placed on the setup of the structural-transient analysis to import the results. Due to this procedure, it is possible to suppress the components of the heating chamber and the supports in the duplicated project so the calculation time is extremely reduced for the structural-transient analysis while the solution of the thermal-transient analysis is still available. It is important to set the source time of the imported component temperatures to all.

2.7.7 Support conditions and convergence behavior

The definition of supports as boundary condition is highly challenging when handling such large surfaces. The main problem is characterized by an achievement of the convergence behavior by the solver, since it is allowed in simulation that the components can penetrate into each other as a function of the contact stiffness. Particularly for components that bend, there is the problem either that the component is not allowed to penetrate far enough into the surface of the support, so the stresses in the component cannot be transferred into deformation, or it penetrates too far and cannot be pushed back. In both cases, the simulation aborts and no sufficient solution is obtained. To solve this problem, first the bottom surface of the brazing assembly is defined as a support only due to compression. This forms an imaginary support plate, where the component is allowed to penetrate it slightly and to lift off from it completely. A manual contact stiffness of 0.1 was defined for this support, and it is crucial to update this factor for each iteration. In addition, the option "weak springs" was activated beyond the gravitational force so the component is restricted from floating into the space. It is highly important to track the computation of the solution when building such a simulation. Therefore, the number of the Newton–Raphson residue and the number of element violations should be set to three within the solution information. This results in a visualization of the last three solution steps before the non-convergent solution. This way, locally unresolvable stress states can be identified and possibly already solved by a refinement of the

local mesh. Furthermore, for large areas, it is essential to manually increase the allowed number of iterations of the solver from fifteen significantly, which is implemented with the APDL-programming command "NEQIT, 100."

3 EXPERIMENTAL RESULTS

In this section, the results of the real brazements are explained.

3.1 Assessment of the initial state

The required roughness of the joining surfaces transverse to the grinding direction of ≤ 6.3 µm could be met and was proofed by three samples of each geometry. Furthermore, the specified evenness of these components below 20 µm could be confirmed by optical 3D measurement. It should be noted that, due to the manual spraying of the scanning spray, a systematic deviation of up to 10 µm is possible, especially at the component edges. The measurements on the residual stress state showed that there are mostly compressive stresses in the range of minus-350 to minus-550 MPa in grinding direction whereby transverse values are lower by more than half.

3.2 Effect of stress relief annealing on the evenness and the residual stress state

No distortion was found for the stress relief annealed samples. Accordingly, this part of the heat treatment is not critical, at least if the stresses present in the as-delivered condition are not exceptionally high. It was proven the residual stresses near the surface could be reduced by half compared to the initial state.

3.3 Distortion of brazed components

For some of the brazements performed, significant component distortion was detected by optical 3D measurement. Figure 3 illustrates the distortion of the brazed component with ID A2 as an example, which showed one of the highest distortion of all samples.

It is clearly visible that the top surface of the brazed component was significantly distorted or respectively bent around the shorter center axis. The negative values result from the best-fit with an ideal CAD-plane. Therefore, the maximum total distortion of sample A2 can be indicated to be about 150 µm. Most of the other samples revealed much less distortion, which, unfortunately, could be not traced back to critical brazing parameters, the cooling mode, or the local position as well.

3.4 Metallographic inspection

The ultrasonic C-Scans of the brazements revealed all the joints of the processes with an overpressure gas cooling were locally insufficient so, e.g., no connection was present in the vicinity of the cooling channel. The analyses of the cross sections for these parts showed the main reason for this was a significant widening of the brazing gap from initially 50 µm up to about 200 mm in the worst case, so there was not enough braze metal to fill up the gap. Due to the morphology of the residues of the braze material, it can be assumed, additionally, there was still a part of the braze in the liquid state. The processes with a heating rate of 50°C/min showed a significantly higher flow behavior of the braze and thus a reduction of the brazing gap to about 25-30 µm compared to the processes with 1 °C/min. Figure 4 illustrates a characteristic joint of sample A1 of the longitudinal edge of the component.

The thickness of the brazed metal was measured to 57 µm, and between the nickel-solid solution phases, there is a continuously pronounced phase band in the center of the joint, which consists of black colored chromium borides and light-gray colored eutectic phases. The formation of these highly brittle phases is generally increasing with the gap size and indicates insufficient temperature-time cycles for diffusion of silicon and boron into the base material.

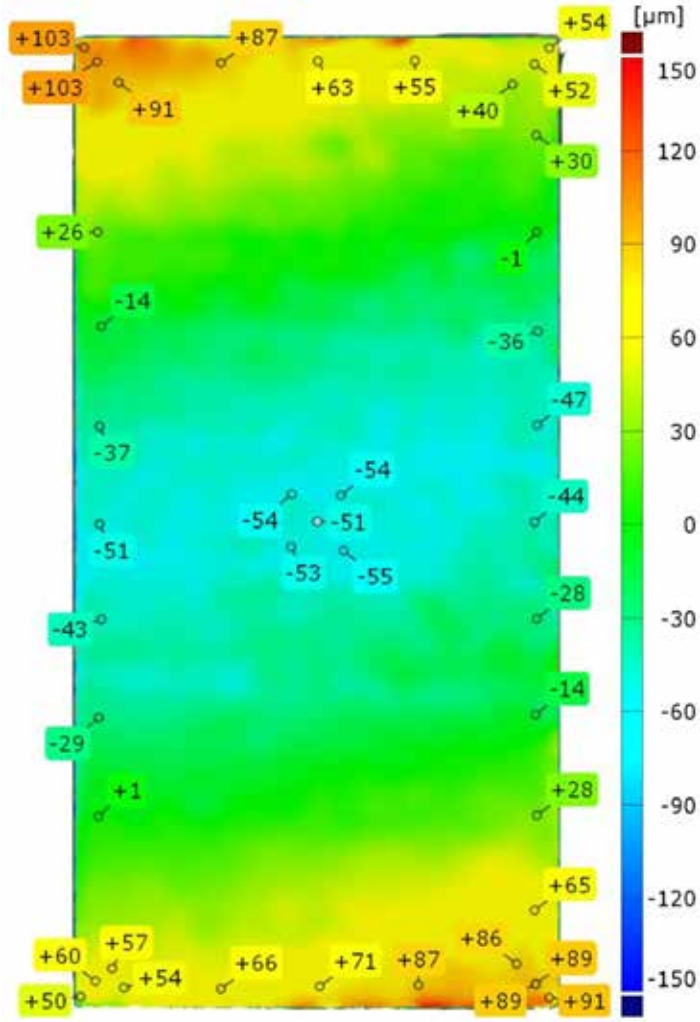

Figure 3: Optical 3D measured distortion of the brazed assembly with ID A2 for the top surface of AISI 316L with a thickness of 5 mm.

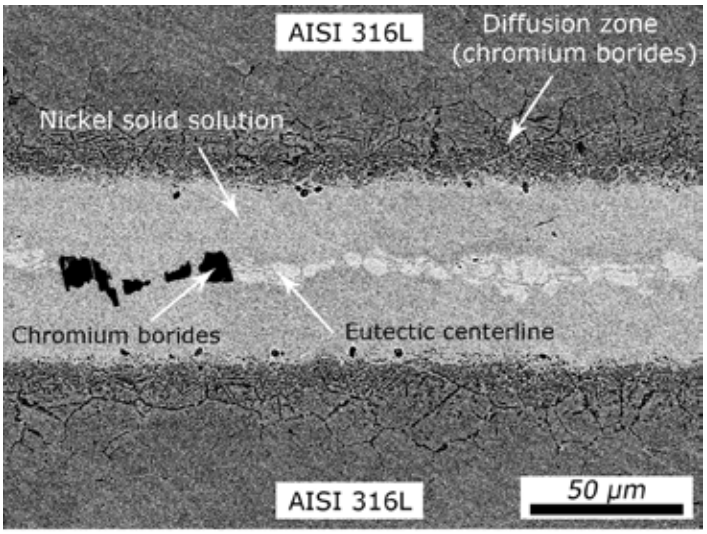

Figure 4: Characteristic SEM image of a brazed joint of sample A1 on the longitudinal edge.

4 SIMULATIVE RESULTS

In this section, the results of the thermal-transient and structural-transient simulations are explained.

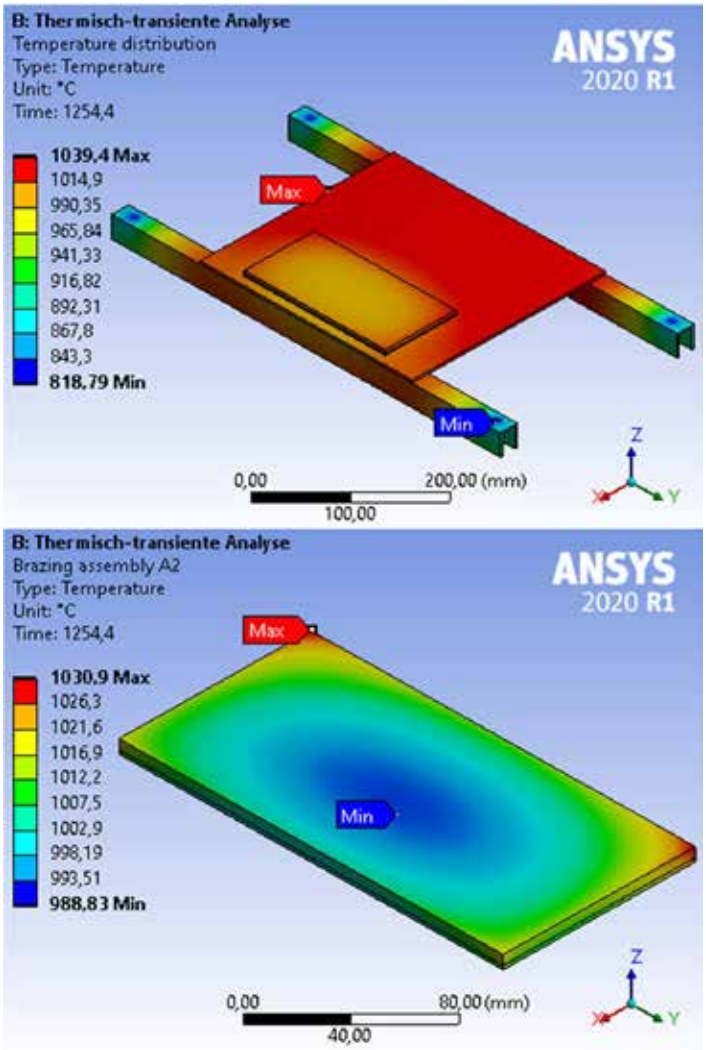

Figure 5: Simulated temperature distribution during heating for the supports and brazing assembly A2.

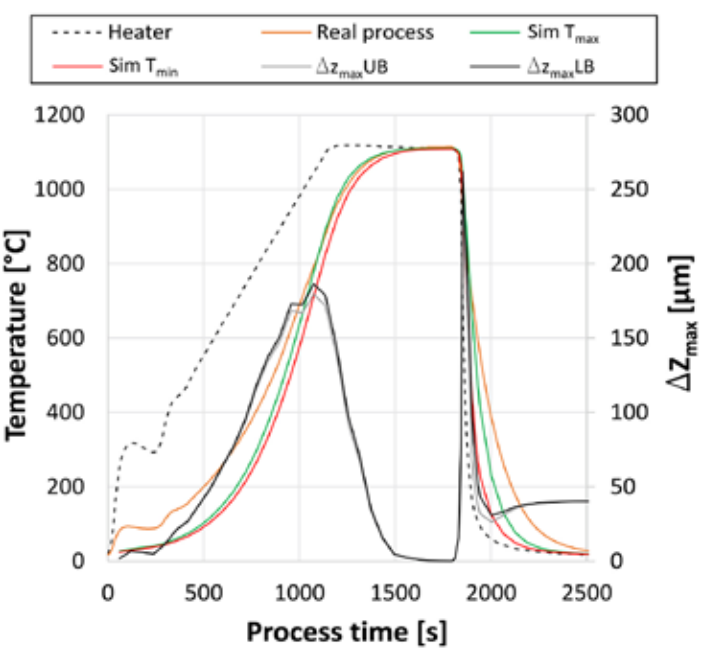

Figure 6: Cycle-dependent distortion Δz_{max} of brazing assembly A2 correlated to real and simulated temperatures.

4.1 Heat distribution in the brazing assembly

The results of the thermal-transient analyses showed a strongly pronounced dependence of the temperature distribution in the brazing assembly on the local component positioning and the process parameter used. The temperature specification of the heating surfaces based on the respective furnace process data from Section 3 represented the real heating behavior of the heating chamber and the components inside quite well, which will be explained in more detail later (Section 5.2). Figure 5 illustrates the temperature distribution during the heating of the brazing assembly, taking into account the surrounding supports (upper image) and of the brazing assembly itself in more detail (lower image).

It was found the four load supports (blanked out) at the end of the U-profiles act as a heat sink. Furthermore, the shading of the brazing assembly due to a partial overlap with the U-profile leads to a stronger heating of the assembly on the opposite side. This is especially the case at the edges that represents the maximum temperature. The temperature field is elliptical with the minimum temperature on the bottom side so a maximum temperature difference of 42°C is present at this time step within the brazing assembly. At the end of the heating, all components of the experimental design were almost completely soaked and corresponded to the heating temperature with a few degrees' deviation. As expected, the largest temperature differences were found in the cooling phase, which will be explained in more detail in the next section.

4.2 Cycle-dependent component distortion

The analyses of distortion in the structural-transient simulation were carried out on the top surface of the upper body (UB) and the lower body (LB) of the brazing assemblies. Therefore, the maximum and minimum of the displacement to the Z-axis, which is normal to the particular surface, were used so that the deformation can be calculated (Δz_{max}) for each step without the effects of general thermal expansion. In addition, these results were correlated manually to the simulated temperatures (max./min.) as well as to the real temperature of the batch thermocouple from the furnace run. Figure 6 shows an exemplarily graph for ID A2.

It can be seen the simulated temperatures overall match the real temperature of the batch quite well, but below 700°C, the deviation was still slightly too large during both heating and cooling. However, it was found that, during heating, the brazing assembly was significantly deformed up to 180 µm, which was completely leveled out at the end of the soaking time. At the beginning of the cooling phase at which the contact was changed to compound, there was sharp increase of deformation up to 250 µm following a brief decrease, but 40 µm distortion remained at the end of the process. Figure 7 shows the results of the thermal-transient and structural-transient analysis for the time step of maximum deformation for brazing assembly A2 during convective cooling.

It is visible that the temperatures at the edges of the brazing assembly were highly decreased to a minimum of 952°C, so a maximum temperature difference of 82°C was present. The maximum temperature was identified in the center of the lower body. The brazing assembly was deformed mainly by bending up from the center point and was especially high at the edges. During further cooling, the local deformation behavior changes from the shown cylindrical one to a finally complete bending around the shorter center axis. Due to the asymmetric temperature field in the brazing assembly, which is produced by a shading effect of the U-profile, a significantly higher distortion of the edges placed on the profile was present compared to the opposite side of the component.

4.3 Final component distortion

In Table 2, the main results of the thermal-transient and structural-transient analyses of the experimental design are summarized.

It is visible that the total calculation time of both analyses (MAPDL-time) was significantly higher for processes using vacuum cooling (VC) due to the very slow cooling rate and the selected step size of 60 s. Processes with convective cooling (N_2) showed very high maximum temperature differences within the brazing assemblies for which the highest values occurred always shortly after the beginning of the cooling. Thus, the maximum interim deformation is pronounced at this time step. As one can see, there are no significant differences in the resulting total deformation of the upper and the lower body (UB, LB). As expected, processes with convective cooling showed significantly higher distortion than processes with vacuum cooling. Furthermore, the simulations with the higher maximum process temperature (1,110°C, ID A2, A3) appeared to have a higher distortion for samples with geometry A than the process with 1,060°C (A6). Furthermore, it was noticeable the temperature differences for geometry B were considerably larger for samples with convective cooling than for samples with geometry A, while the resulting distortion is lower. Based on these two relationships, it can be concluded material thickness has a significant influence on distortion. In addition, it could be shown by comparison of A2 and A3 that the local position of the brazing assembly affects the distortion as well.

5 COMPARISON OF EXPERIMENTAL AND SIMULATIVE RESULTS

In this section, the results of the experimental and simulation will be compared. Afterwards, the main actuating values will be explained to apply the FE-model closer to reality and to adjust the FE-model toward a truthful depiction of the actual distortion.

5.1 Reality comparison

A superior goal of a simulation is always given by the experimental verification. The simulation results revealed the influences of the varied parameters from the experimental design in high detail. As mentioned before, the distortion of the real brazements does not match with the expectation of the effect of the varied parameters very well. Therefore, an intensive comparison is not useful at the current stage of development. Figure 8 illustrates the final distortion of sample A2 of 40 µm, which was not matching numerically but geometrically pronounced in a similar way to the results of the optically 3D measured real sample shown in Figure 3 (150 µm distortion).

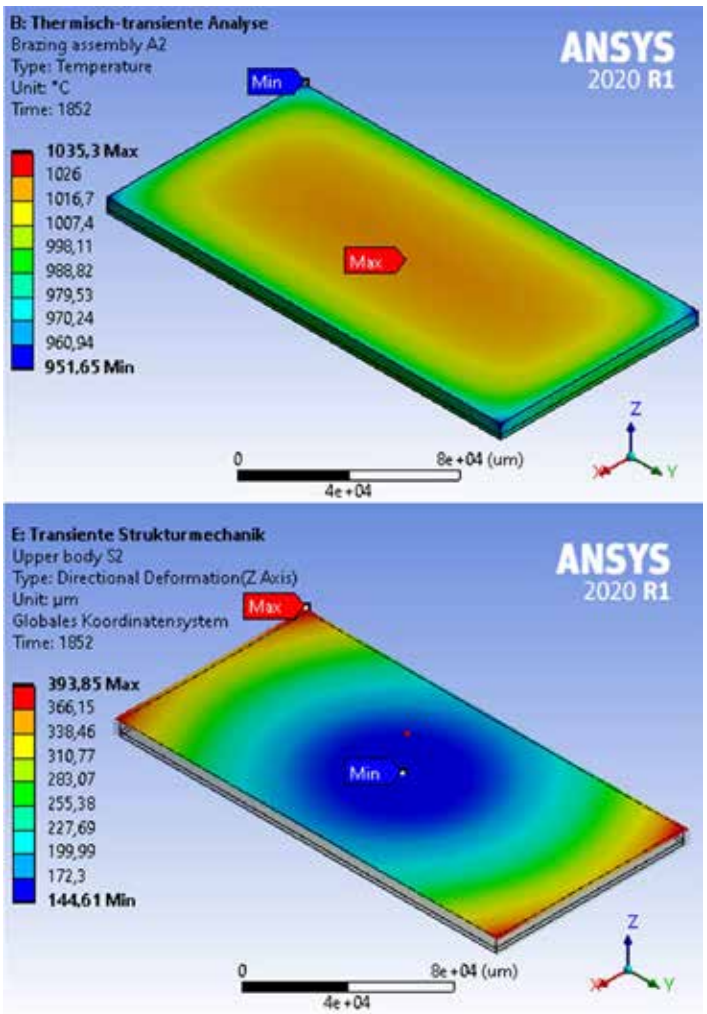

Figure 7: Temperature distribution and interim deformation Δz_{max} of brazing assembly A2 at time step with max. deformation during convective cooling.

5.2 Actuating variables of the FE-model

A detailed analysis of the achieved results revealed actuating variables of the FE-model, which were used to improve the simulation results and to reduce the calculation times. The two most important values are characterized by the emissivity of the materials and by the heat transfer coefficient. Both parameters are to be defined temperature-dependent and enable, with some iterative effort, a perfect match of the temperature cycle of the batch thermocouple of real furnace runs.

Geometry and ID	Process time [s]	Cooling mode	MAPDL-time [h:min]	ΔT_{max} Sim. [°C]	Interim Δz_{max} [µm]	Final Δz_{max} *UB* [µm]	Final Δz_{max} *LB* [µm]
A1	39,312	VC	44:02	19	55	8	8
A2	3284	N_2	11:16	223	262	40	40
A3	3005	N_2	9:35	225	255	33	33
A4	54,867	VC	42:35	18	55	8	8
B1	4446	N_2	12:24	374	207	22	23
B2	65,629	VC	52:22	77	61	0	0
B3	50,561	VC	45:04	73	61	0	0
B4	4441	N_2	11:39	383	193	21	23
A5	42,819	VC	43:10	35	94	8	8
A6	5077	N_2	14:00	213	203	29	29
B5	65,321	VC	53:12	115	84	0	0
B6	7336	N_2	14:28	367	169	24	21

Table 2: Main results of the simulation analyses.

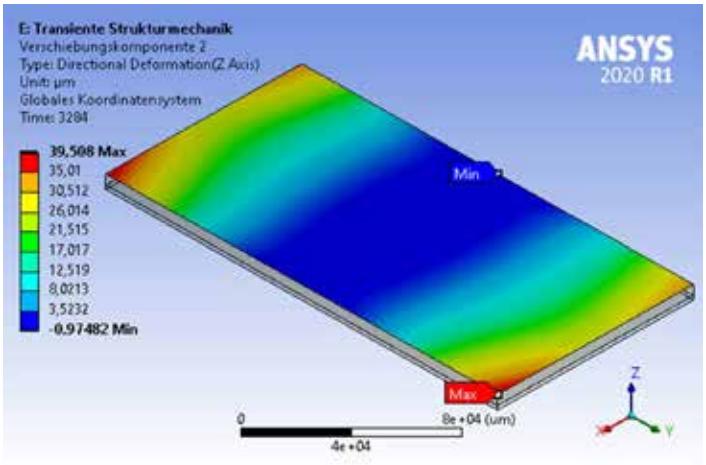

Figure 8: Final deformation Δz_{max} of brazing assembly A2.

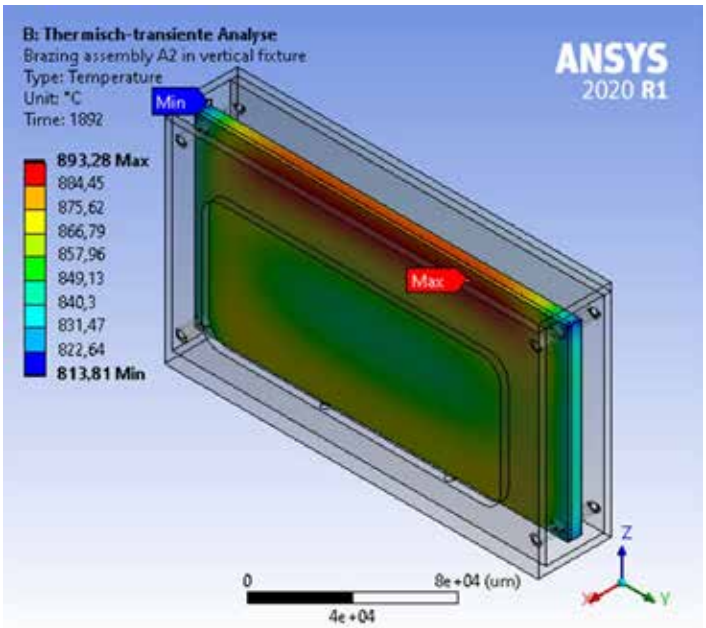

Figure 9: Temperature distribution of brazing assembly A2 at step with max. temperature difference during convective cooling in a vertical fixture.

Another important value was identified by the radiation of the outer part of the load supports by which the amount of heat dissipated from the adiabatic chamber can be additionally regulated. It should be mentioned that the emissivity and the heat-transfer coefficient are difficult to determine experimentally and mostly dependent on many further factors, so they can be varied within a relatively wide range. In order to increase the calculation time, the mesh size of the brazing filler metal and AISI 316L for geometry A was doubled to 3.0 mm. In addition, the step size was decoupled to 600 seconds for processes with vacuum cooling and temperatures below 400°C in load step three. The results of these parameter adjustments are marked in Table 3 by a star and are compared to the results of the previous simulation results.

It is visible that the calculation times were significantly reduced for all processes. For those processes with convective cooling (N_2), the maximum temperature difference in the brazing assemblies was also decreased, and thus, the final distortion improved substantially. For the processes with vacuum cooling, no significant difference was noticeable.

5.3 Adaptive distortion minimization

To give an outlook on the usability of the simulation, a vertical fixture was developed based on the simulation results of ID A2*, illustrated in Figure 9.

The fixture of material AISI 316L is designed to have as little contact as possible with the brazing assembly, which is placed on two tips on the bottom and aligned by four tips from each side. The scale of the open area at the sides was derived from the temperature distribution of the brazing assembly of the previous simulations so the edges are shaded to the radiation during heating and protected by the cool gas flow in reality. Since the simulation does not consider this flow until now, the emission on the edges during cooling is reduced by the hot face of the fixture. Compared to the corresponding simulation A2*, the vertical fixture reduced the maximum temperature difference in the brazing assembly from 141 to 79°C, the interim max. distortion from 275 to 31 µm, and the final maximum distortion from 14 to 8 µm.

6 SUMMARY, CONCLUSION, AND OUTLOOK

In this study, a new method of radiation and contact modeling was developed to identify the most critical influencing factors of distortion for vacuum brazed assemblies with simulation.

The results obtained are summarized in the following:

›› The new method of radiation modeling enables the import of real furnace temperature data to be used for the heater in the simulation.

›› The contact modeling developed and the boundary conditions used both reliably solved the convergence problem of distortion calculation of large area and thin components and enabled a free positioning of one or more components in the heating chamber.

›› The emissivity and the heat transfer coefficient were identified as actuating variables to adjust the heating and cooling behavior of

Geometry and ID	Process time [s]	Cooling mode	MAPDL-time [h:min]	ΔT_{max} Sim. [°C]	Interim Δz_{max} [µm]	Final Δz_{max} *UB* [µm]	Final Δz_{max} *LB* [µm]
A2	3284	N_1	11:16	223	262	40	40
A2*	3284	N_1	2:36	141	275	14	14
A5	42,819	VC	43:10	35	94	8	8
A5*	42,819	VC	5:14	34	94	8	8
A6	5077	N_2	14:00	213	230	29	29
A6*	5077	N_2	3:26	141	203	11	12
B5	65,321	VC	53:12	115	84	0	0
B5*	65,321	VC	20:01	115	86	0	0
B6	7336	N_2	14:28	367	169	24	21
B6*	7336	N_2	10:13	245	176	18	11

Table 3: Effect of parameter adjustments (*).

the FE-model to the real vacuum furnace.

Distortion was mainly built shortly after the contact was changed to a bond when the temperature difference within the brazing assembly exceeds the yield strength at the initially high cooling rates even if vacuum cooling is used. Since the yield strength of AISI 316L above 870°C is very low and difficult to determine accurately, the definition of this temperature-dependent data set can be considered as a crucial factor for the simulation results.

With further cooling, a considerable amount of the deformation was leveled out with the shrinkage of the component. If the interim deformation was too high, the brazed assembly will remain distortion, which depended furthermore on the material thickness.

A fixture for a vertical positioning of the component reduced the maximum temperature difference in the brazing assembly from 141 to 79°C, the maximum interim distortion from 275 to 31 µm, and the final distortion from 14 to 8 µm.

Thus, the developed model is able to investigate the effect of different cooling rates on the final distortion for an individual geometry and positioning of the brazing assembly in future.

Based on the results obtained, it is highly recommended to investigate a controlled cooling rate (e.g., 10°C/min) up to 900°C heater temperature and then overpressure gas cooling for AISI 316L to avoid the formation of the σ-phase. For further development of the FE-model, it should be possible to take the residual stresses into account, ideally with depth resolution, which are suspected to be responsible for the non-systematic distortion results of the real brazements. In addition, it might be beneficial to implement a computational fluid dynamics (CFD) simulation for the processes using overpressure gas cooling instead. However, all these efforts are expected to highly increase the calculation times of the simulation.

DATA AVAILABILITY

The project data and material is stored in accordance with the guidelines of the German Federation of Industrial Research Associations and can be made available on request.

CODE AVAILABILITY

The simulation data can be provided upon personal request.

ACKNOWLEDGEMENTS

Many thanks to Fabian Maaß from the Institute of Forming Technology (IUL) at TU Dortmund University for the machine time and the support of the 3D measuring system GOM ATOS II Triple Scan.

FUNDING

Open Access funding enabled and organized by Projekt DEAL. Many thanks to the German Federation of Industrial Research Associations (AiF) for the financial support of project 21.960N "Investigation and simulation of the heat input into vacuum brazed components to reduce distortion of large joint surfaces."

PUBLISHER'S NOTE

Springer Nature remains neutral with regard to jurisdictional claims in published maps and institutional affiliations.

REFERENCES

[1] Wan Y, Jiang W, Dong Z et al (2023) Brazing manufacturing technology of plate-fin heat exchanger for solid oxide fuel cells. Int J Hydrog Energy 48:4456–4468.

[2] Luo Y, Li ZH, Luo YZ et al (2023) Vacuum brazing effect on the interlayer failure behavior of TiAl/GH3536 hetero-thin-walled structure with BNi-2 interlayer. Thin Wall Struct 184:110492.

[3] Jiang WC, Gong JM, Tu SD et al (2009) Modelling of temperature field and residual stress of vacuum brazing for stainless steel plate-fin structure. J Mater Process Technol 209:1105–1110.

[4] Jiang WC, Gong JM, Tu SD et al (2009) Three-dimensional numerical simulation of brazed residual stress and its high-temperature redistribution for stainless steel plate-fin structure. Mater Sci Eng A 499:293–298.

[5] Ma S, Li B, Zhang P et al (2022) Effect of brazing filler metals and welding parameters on laser welding-brazing joints of WC-Co to S1045. Metals 12:1780.

[6] Chiocca A, Frendo F, Bertini L (2019) Evaluation of heat sources for the simulation of the temperature distribution in gas metal arc welded joints. Metals 9:1142.

[7] Lou M, Cai W, Huang J et al (2020) Simulation of laser brazing of sheet panels and parametric studies of thermally-induced distortion reduction. JMP 60:1–10.

[8] Amelzadeh M, Mirsalehi SE (2019) Dissimilar vacuum brazing of cemented carbide to steel using double-layer filler metals. JMP 47:1–9.

[9] Kahlol KK, Aldhaidhawi M, Nawi SA (2021) Simulation between soldering and brazing of copper at 450 temperature by Zn-Sn fillet alloy. IOP Conf Series: Mater Sci Eng 1076:012074. https://doi.org/10.1088/1757-899X/1076/1/012074.

[10] Li P, Yan Y, Ba J et al (2023) The regulation strategy for releasing residual stress in ceramic-metal brazed joints. JMP 85:935–947.

[11] Yi R, Chen C, Li Y et al (2021) Research advances in residual thermal stress of ceramic/metal brazes. Ceram Int 47:20807–20820.

[12] Barrena MI, Gómez de Salazar JMN, Gómez-Vacas M (2014) Numerical simulation and experimental analysis of vacuum brazing for steel/cermet. Ceram Int 40:10557–10563.

[13] Qin G, Su Y, Meng X et al (1925) 2015 Numerical simulation on MIG arc brazing-fusion welding of aluminum alloy to galvanized steel plate. Int J Manuf Technol 78:1917.

[14] Guo S, Sun L, Fang J et al (2022) Residual stress, microstructure and corrosion behavior in the 316L/Si3N4 joint by multi-layered braze structure-experiments and simulation. Ceram Int 48:32894–32907.

[15] Bartout D, Süleymanov N (2017) Simulation methods for joining of tools with complex geometries by brazing. J Mater Environ Sci 8:4415–4425.

[16] Brzoza M, Pietzsch R, Kaymak Y et al (2005) Minimizing the distortion of steel profiles by controlled cooling. Steel Res Int 76:399–407.

[17] Liu G, Wang A, Tang R et al (2022) Fabrication and modeling of ultra-hard and high-strength B4C-based laminated ceramics by brazing joining. Ceram Int 48:27982–27987.

[18] Wang Y, Liu M, Zhang H et al (2021) Fabrication of reliable ZTA composite/Ti6Al4V alloy joints via vacuum brazing method: Microstructural evolution, mechanical properties and residual stress prediction. J Eur Ceram 41:4273–4283.

[19] Jing Y, Xiong H, Shang Y et al (2020) Simulation on Ti-based filler and vacuum brazing for TA15 alloy. Weld World 64:1261–1268.

[20] Jafari A, Sadeghianjahromi A, Wang C-C (2022) Experimental and numerical investigation of brazed plate heat exchangers - A new approach. Appl Therm Eng 200:117694.

[21] Zhang Y, Chen Y, Zhou J (2000) Experimental and numerical study on microstructure and mechanical properties for laser welding-brazing of TC4 Titanium alloy and 304 stainless steel with Cu-base filler metal. J Mater Res Technol 9:465–477.

[22] Zouaghi A, Velay V, Soveja A et al (2016) A multi-scale approach to investigate the nonlinear subsurface behavior and strain localization of X38CrMoV5-1 martensitic tool steel: Experiment and numerical analysis. Int J Plast 87:130–153.

[23] Deile J, Doberitzsch J (2013) Essential building blocks for a flexible approach to laser source design, Proc. SPIE 8603, High-Power Laser Materials Processing: Lasers, Beam Delivery, Diagnostics, and Applications II, 860309. https://doi.org/10.1117/12.2006068.

[24] Aranaga S, Izcara J, Del Río L et al (2016) Thermal modelling of a brazing process of vacuum interrupters. 2016 27th International Symposium on Discharges and Electrical Insulation in Vacuum (ISDEIV), Suzhou, China, p 1–4. https://doi.org/10.1109/DEIV.2016.7763943.

[25] Zhao XF, Wimmer A, Zaeh MF (2023) Experimental and simulative investiga-

tion of welding sequences on thermally induced distortions in wire arc additive manufacturing. Rapid Prototyp J 29:53–63.

[26] Zaharinie T, Yusof F, Hamdi M et al (2014) Effect of brazing temperature on the shear strength of Inconel 600 joint. Int J Adv Manuf Technol 73:1133–1140.

[27] Ivannikov A, Krasnova E, Penyaz M (2020) Effect of high-temperature brazing with a nickel-based STEMET 1301A brazing alloy on the unbrazing temperature of 12Kh18N10T steel joints. Int J Adv Manuf Technol 110:1319–1326.

[28] Tillmann W, Henning T, Boretius M (2019) Effect of the dwell time on the microstructure and tensile strength of vacuum-brazed tool steels using BNi-2 filler metal. Weld world 63:1477–1488.

[29] Mann B, Ford K, Neilsen M et al (2020) Minimizing residual stress in brazed joints by optimizing the brazing thermal profile. Proceedings of the ASME 2020 International Mechanical Engineering Congress and Exposition. Volume 2A: Advanced Manufacturing. Virtual, Online. November 16–19. https://www.osti.gov/servlets/purl/1812850.

[30] Heuer V, Leist T, Schmitt G (2016) Distortion control through synchronized vacuum heat treatment. HTM J Heat Treatm Mat 71:83–89.

[31] Since JJ, Irretier O (2010) Vacuum heat treatment and high pressure gas gas quenching - Aspects in Distortion Control. Heat Processing 8:1–6.

[32] Kallmeyer R (2006) Untersuchungen zur Strahlungsmodellierung in ANSYS, TU Ilmenau, GRIN Verlag. https://www.grin.com/document/79513.

[33] Tennenhouse CC (1971) Control of Distortion During the Furnace Cycle is vitally important for successful brazing, particularly of complex parts and assemblies. AWS Welding J October.

[34] American Iron and Steel Institute (2020) High-temperature characteristics of stainless steels - A designers' handbook series No. 9004. https://nickelinstitute.org/media/4657/ni_aisi_9004_hightemperaturecharacteristics.pdf.

[35] Richter F (2011) The physical properties of steels "The 100 steels program" part I: Tables and figures, TU Graz, Institute of experimental physics. https://www.tugraz.at/institute/iep/forschung/thermophysics-and-metalphysics/literature/.

[36] Gardner L, Ashraf M (2010) Elevated temperature material properties of stainless steel alloys. J Constr Steel Res 66:634–647.

[37] Ding J, Han EH, Zhang Z et al (2017) Influence of sigma phase on corrosion behavior of 316L stainless steel in high temperature and high pressure water, Mater. at. High Temp 34:78–86.

[38] Lescur A, Stergar E, Lim J et al (2021) Microstructural investigation and identification of intermetallic σ-phase in solution annealed 316L-type austenitic stainless steel. Mater Charact 182:111524.

[39] Aditya DM, Ardy H, Lantang YSF et al (2023) The study of sigma and carbide in cast austenitic stainless-steel grade HH after 24 years of high-temperature service. Heliyon 9:e14109.

[40] Andreatta F, Lanzutti A, Revilla RI et al (2022) Effect of Thermal Treatment on Corrosion Behavior of AISI 316L Stainless Steel Manufactured by Laser Powder Bed Fusion. Materials 15:6768.

[41] Laleh M, Hughes AE, Xu W et al (2019) On the unusual intergranular corrosion resistance of 316L stainless steel additively manufactured by selective laser melting. Corros Sci 161:108189.

[42] Böhler Edelstahl GmbH (2006) Praxis-Service - Erfolgreiche Edelstahlverarbeitung. https://docplayer.org/22768989-Praxis-service-erfolgreiche-edelstahlverarbeitung.html.

ABOUT THE AUTHORS

Wolfgang Tillmann, Tim Henning, Lukas Wojarski, Christian Timmer, and Finn Ontrup are with the Institute of Materials Engineering, TU Dortmund University. This article has been edited to conform with the style of Thermal Processing.

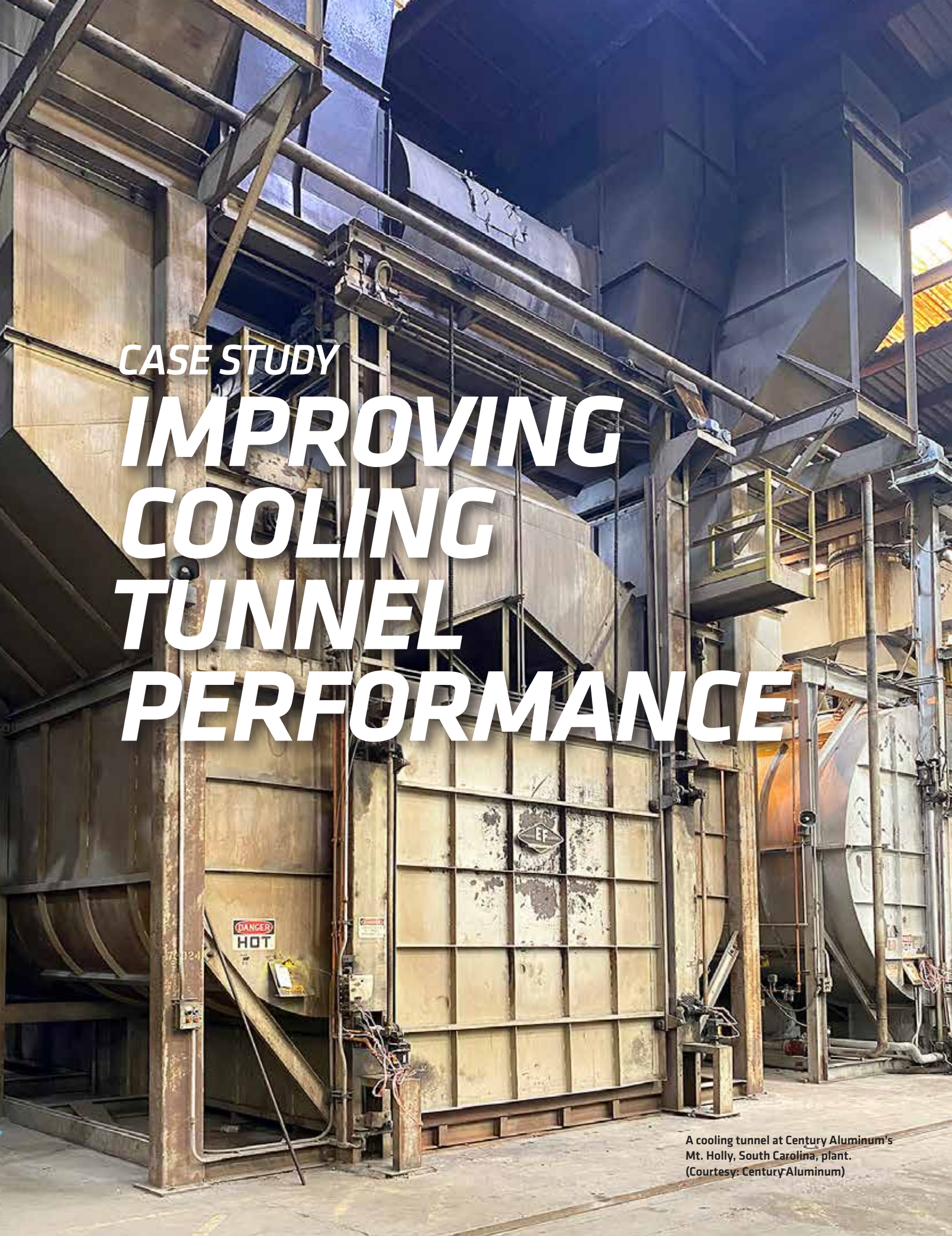

A cooling tunnel at Century Aluminum's Mt. Holly, South Carolina, plant. (Courtesy: Century Aluminum)

CASE STUDY

IMPROVING COOLING TUNNEL PERFORMANCE

Aluminum caster upgrades its Mt. Holly facility with drive hardware, PLC-to-internet gateway, and data analysis, which increased the company's uptime by more than 50%.

By JACKIE STOKES

The Mt. Holly, South Carolina, smelting facility of global producer Century Aluminum houses casting equipment to process nearly 230,000 metric tons of material into standard-grade ingot, HDC ingot, extrusion billet, and other products. As the first primary aluminum plant in the world to achieve the ISO 9001 Quality System Standard, Mt. Holly has the highest standards for production efficiency, energy utilization, and environmental control.

Recently, the company was faced with an increase in downtime to its two cooling tunnels due to legacy controls going beyond their functional limits.

"The older drives would have required major rebuilding as they were able to track only speed, delivering the data to the PLC," said Cast House Technician Sam Wilson. "We required more data and faster processing of it."

These tunnels are used for cooling aluminum billets after they've been homogenized, reducing the temperatures typically from 1,000°F to 90°F. The drives on these units control the main fans to bring cool air to the loads and circulate it throughout the aluminum bundles. The cooling cycle averages to about a four-hour cool-down time.

"In full operation now, the new Siemens control system is allowing a cooling scenario at Mt. Holly on a 150-ton load in half the time as previously required, which translates to 300,000 more pounds of aluminum per day processed," Wilson said. "We are very pleased with the improved performance we're getting from the Siemens controls."

IMPROVEMENTS BEGIN

Wilson contacted Miguel Ortiz, product manager at Electrical Equipment Company, a local distributor, who represents Siemens in the area. Ortiz and his team, Outreach Resources, did an assessment of the situation and devised a solution that met and exceeded Wilson's expectations. The new drive and communications system involved the retrofit of a competitor's drive with a Siemens SINAMICS G120 drive, an intelligent operator panel (IOP-2), and a unique Remote I/O (RIO) to EtherNet/IPTM gateway, co-designed by Siemens and SoftPLC. This device is specifically designed to enable easy migration from the legacy drives to the new drives, plus the data transmitted now includes current and torque, a significant advantage for the customer.

The results of this improvement, according to the team at Century Aluminum, included a tracked reduction in downtime of more than 50 percent, which enables more reliable cooling of the aluminum materials, proper data analysis due to additional electrical information being transmitted and programs being saved on the IOP-2 for faster recovery. With no tools required to wire one drive to another, due to the plug-and-play feature, significant time was saved in the implementation of the new hardware.

"This upgrade truly brought our casting house into the modern age," Wilson said.

Ortiz further detailed the upgrade.

The cooling tunnel 150 hp drives cabinets before conversion. (Courtesy: Century Aluminum)

"One of the big advantages on this job is that we were able to take a demo unit into Mt. Holly and show Sam and his team how to configure the gateway without disconnecting the legacy PLC-5 controller," he said. "We could scale, readjust, and map the start/stop activity, plus being able to install and test run the new equipment without changes to the PLC-5 controller program meant the system on the first retrofitted cooling tunnel were ready to roll much faster and at a lower overall cost."

SMOOTH CHANGES

Since these cooling tunnels run 24/7, 365 days a year, according to Wilson, it was critical the changeovers be as smooth as possible. In fact, Ortiz said both control cabinets were done in eight hours.

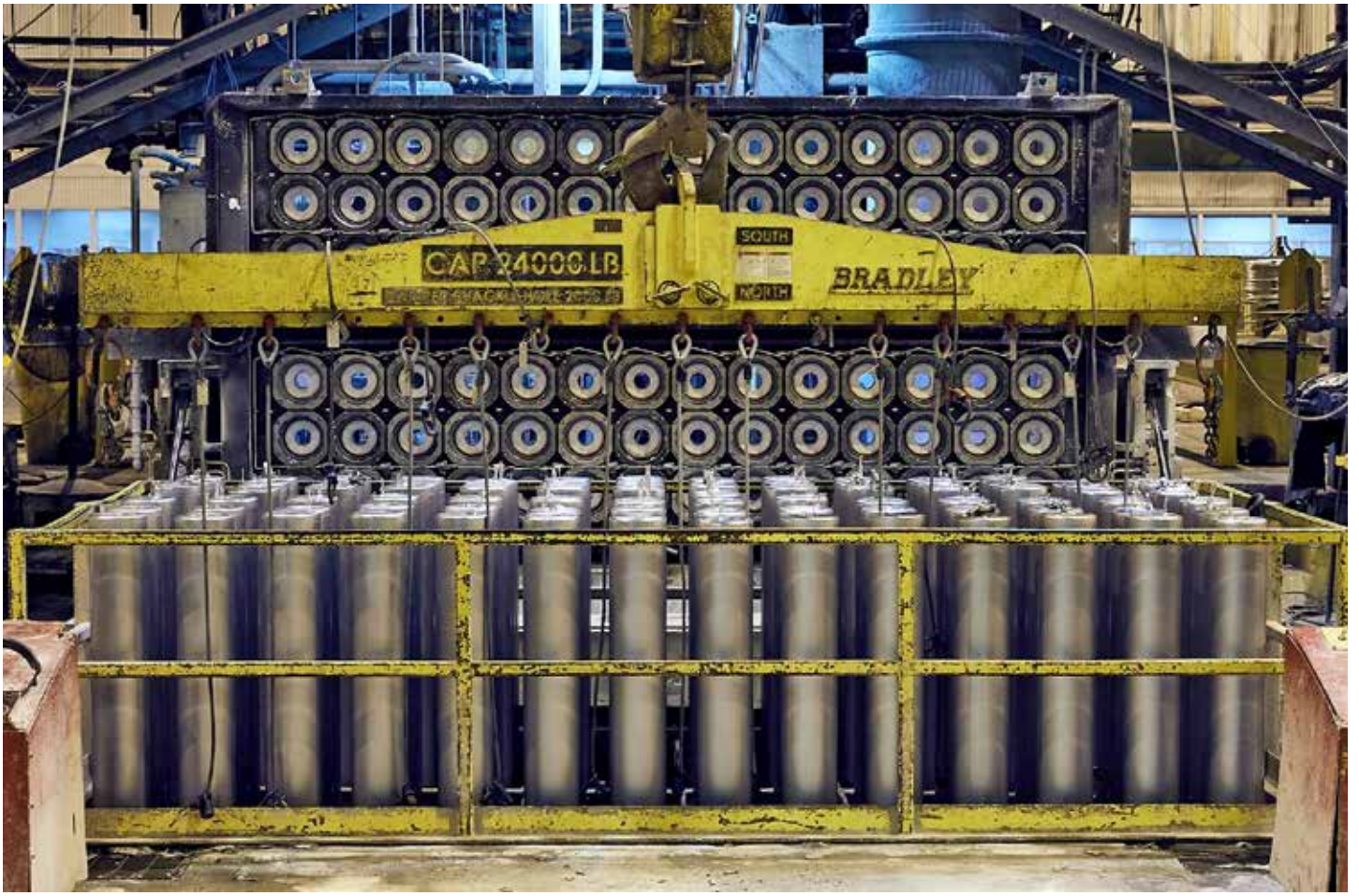

Century Aluminum's Mt. Holly plant produces about 70 alloy combinations, with custom ordering available, including billet, horizontal direct chill (HDC) ingot, T-ingot, and slab aluminum. (Courtesy: Century Aluminum)

Using the IOP-2 and its memory for programs, Wilson and his team can use the Siemens Totally Integrated Automation (TIA) Portal to further minimize downtime, as the tunnel performance can be set to ramp up per the known batch of incoming product.

In full operation now, the new Siemens control system is allowing a cooling scenario on a 75-ton load in half the time as previously required, which translates to 300,000 more pounds per day processed.

As a further energy saving, the motors on the tunnel conveyors now operate more efficiently in a standard vs. dynamic mode.

"With the legacy drives, we got only the current data back to the PLC," Wilson said. "On the IOP-2, we get to see real-time, current, RPM, and the DC output. If there's something wrong, we know it immediately and can initiate corrective action."

An additional inventory advantage was also cited by Wilson, as the 150 hp drives can be purposed for use in the carbon plant run by Century, also located in Mt. Holly, where 75 hp is the standard motor in use.

TRAINING

"In addition to the demo unit we used, about 10 days prior to the install, we did an event at the customer's facility where we gathered the technicians and some of the engineers to give them an overview of the drives, the IOP-2, and how to troubleshoot from the TIA Portal software," Ortiz said. "The training gave them both practical knowledge and a higher comfort level, as the majority of those present had lots of experience with another brand of drive products. We were able to show them how to seamlessly connect the new and the remnant legacy products."

Ortiz also complimented the Century team for going the extra mile to take the maintenance and management classes Siemens offers.

Overall, the conversion on this application took less than 60 days.

"The plug-and-play technology plus the substantial program storage on the IOP-2 make our training of younger techs and operations personnel much easier," Wilson said. "With the older equipment, line code upgrades were very time-consuming, while they're automatic on the Siemens equipment. The younger employees have that fast and easy modular mindset, which is great, as it matches the plug-and-play technology, and it saves us a lot of time and money. I thankfully was on an old boat in the Navy and some old Los Angeles class submarines, so I know a bit more about the history of the legacy gear."

Through these and other advancements made in recent years, the Century Aluminum's Mt. Holly plant has become an industry leader, something Wilson and his team are proud to say. The plant currently produces about 70 alloy combinations, with custom ordering available. It also produces billet, horizontal direct chill (HDC) ingot, T-ingot, and slab aluminum. In addition to that, Century Aluminum operates a carbon anode plant that has begun using Siemens controls.

ABOUT THE AUTHOR

Jackie Stokes is a marketing programs manager in the Siemens Motion Control business. With 15 years' experience in industrial automation, she started her career at Rockwell Automation and held roles in manufacturing, engineering, sales, and marketing. Stokes holds a BS in mechanical engineering from Purdue University and an MBA from the University of Nebraska-Lincoln.

The cooling tunnel fan cabinet with Siemens SINAMICS G120 drive installed. (Courtesy: Century Aluminum)

REIMAGINING THE STEEL PRODUCTION PROCESS

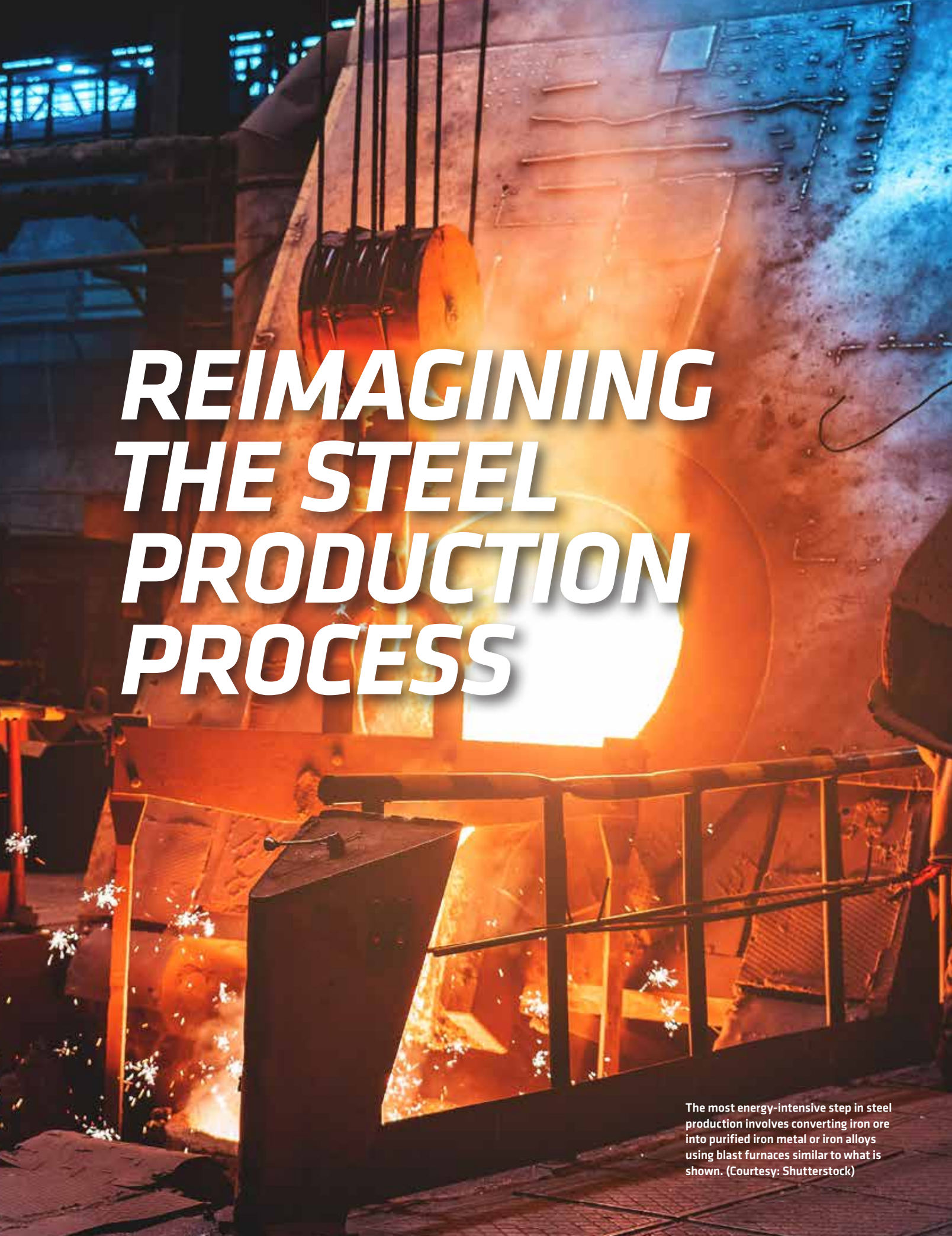

The most energy-intensive step in steel production involves converting iron ore into purified iron metal or iron alloys using blast furnaces similar to what is shown. (Courtesy: Shutterstock)

The Department of Energy funds new center that will develop a cost-effective method for decarbonized manufacturing for steelmaking without a blast furnace.

By JOSEPH E. HARMON

Steel has a major impact on everyone's lives and our economy. It is crucial to cars, trucks, airplanes, buildings, and more. However, there is a significant issue with its production process. Globally, it accounts for a large percentage of greenhouse gas emissions from the industrial sector.

The U.S. Department of Energy (DOE) recently announced $19 million in funding more than four years for DOE's Argonne National Laboratory to lead the multi-institutional Center for Steel Electrification by Electrosynthesis (C-STEEL). The center's charge is to develop an innovative and low-cost process that would replace blast furnaces in steelmaking and reduce greenhouse gas emissions by 85 percent.

"It's a big target that has a high reward if successful," said Brian Ingram, the C-STEEL director and an Argonne group leader and materials scientist.

CUTTING EMISSIONS

C-STEEL is a key project of the DOE's Industrial Heat Energy Earthshot initiative, which aims to significantly cut emissions from the energy-intensive process of industrial heating. Partners in the center include Oak Ridge National Laboratory, Case Western Reserve University, Northern Illinois University, Purdue University Northwest and the University of Illinois Chicago.

The most energy-intensive step in steel production involves converting iron ore into purified iron metal or iron alloys using blast furnaces. This demands temperatures of 2,500 to 2,700 degrees Fahrenheit, hotter than an erupting volcano. The center's target is to develop a process that will essentially eliminate that heat demand, achieving an 85 percent reduction in greenhouse gas emissions by 2035.

"While current steelmaking requires intense heat from blast furnaces, our electrodeposition process will need low or even no heat input at all," Ingram said. "It will also be cost efficient and adaptable to industrial-scale operations."

The electrodeposition process involves dissolving iron ore in a solution and using electricity to initiate a reaction that deposits a useable iron metal or alloy for steelmaking. The solution is a liquid electrolyte similar to those found in batteries.

"We will be building upon the immense knowledge base we gained about different battery electrolytes from the work done by the Joint Center for Energy Storage Research, led by Argonne," Ingram said.

THREE-PART PROJECT

The project has three thrusts. Two of them will investigate different processes for electrodeposition. One process will operate at room temperature using water-based electrolytes. The other will use a salt-based electrolyte and will function at temperatures 1,800 to 2,000 degrees Fahrenheit below current blast furnaces. The energy for this process is low enough that it could be provided by renewables or waste heat from a nuclear reactor.

A third thrust will focus on gaining an atomic-level understanding of each process. The goal of this thrust is to exert precise control over both the structure and composition of the metal products so they can be incorporated into existing downstream processes of steelmaking.

Each thrust will incorporate an artificial intelligence-based platform to ensure a unified approach to electrolyte design. To that end, C-STEEL will be drawing upon the world-class computational resources of two Leadership Computing Facilities, one at Argonne and the other at Oak Ridge. Both are DOE Office of Science user facilities.

C-STEEL is a key project of the DOE's Industrial Heat Energy Earthshot initiative, which aims to significantly cut emissions from the energy-intensive process of industrial heating. (Courtesy: Argonne National Laboratory)

PRACTICAL APPLICATIONS

C-STEEL will also take advantage of the materials characterization capabilities of two other DOE user facilities at Argonne, the Advanced Photon Source and the Center for Nanoscale Materials. The center focuses on basic energy research while aiming to ensure its findings will support eventual practical applications.

"Another key part of the center is that one of the partner universities is a minority-serving institution, the University of Illinois Chicago," Ingram said. "Through their participation and other actions, we will

be forming a diverse team to contribute to our research efforts."

C-STEEL also plans to implement outreach initiatives, mentorship programs, and career development opportunities for students and postdocs to excite the next generation of scientists.

This research is being funded by the DOE's Office of Science, Basic Energy Sciences and Advanced Scientific Computing Research.

ABOUT ARGONNE'S CENTER FOR NANOSCALE MATERIALS

The Center for Nanoscale Materials is one of the five DOE Nanoscale Science Research Centers, premier national user facilities for interdisciplinary research at the nanoscale supported by the DOE Office of Science. Together the NSRCs comprise a suite of complementary facilities that provide researchers with state-of-the-art capabilities to fabricate, process, characterize, and model nanoscale materials, and constitute the largest infrastructure investment of the National Nanotechnology Initiative. The NSRCs are located at DOE's Argonne, Brookhaven, Lawrence Berkeley, Oak Ridge, Sandia, and Los Alamos National Laboratories. For more information about the DOE NSRCs, go to science.osti.gov/User-Facilities/User-Facilities-at-a-Glance.

The Argonne Leadership Computing Facility provides supercomputing capabilities to the scientific and engineering community to advance fundamental discovery and understanding in a broad range of disciplines. Supported by the U.S. Department of Energy's (DOE's) Office of Science, Advanced Scientific Computing Research (ASCR) program, the ALCF is one of two DOE Leadership Computing Facilities in the nation dedicated to open science.

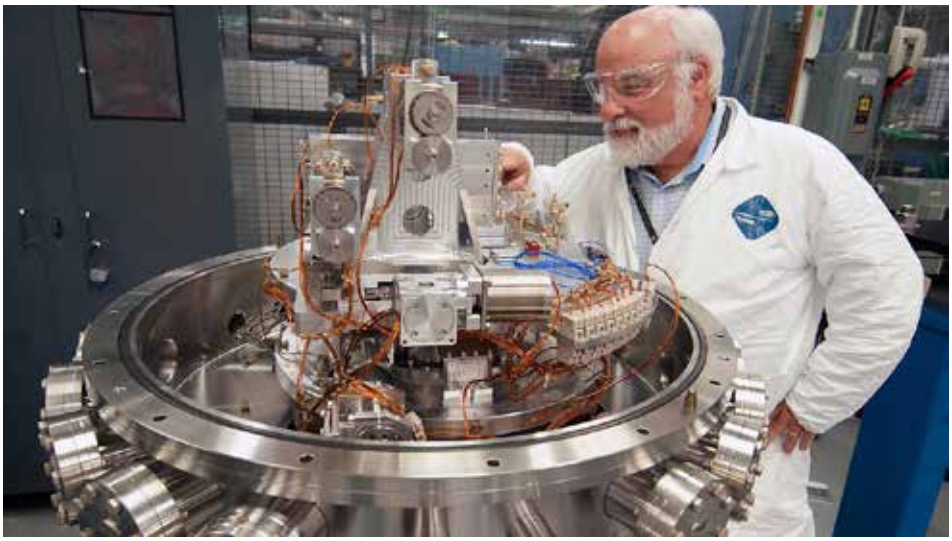

The Advanced Photon Source (APS) at Argonne National Laboratory is one of the world's most productive X-ray light source facilities. The APS provides high-brightness X-ray beams to a diverse community of researchers in materials science, chemistry, condensed matter physics, the life and environmental sciences, and applied research. (Courtesy: Argonne National Laboratory)

Argonne National Laboratory seeks solutions to pressing national problems in science and technology. The nation's first national laboratory, Argonne conducts leading-edge basic and applied scientific research in virtually every scientific discipline.

ABOUT THE ADVANCED PHOTON SOURCE

The U. S. Department of Energy Office of Science's Advanced Photon Source (APS) at Argonne National Laboratory is one of the world's most productive X-ray light source facilities. The APS provides high-brightness X-ray beams to a diverse community of researchers in materials science, chemistry, condensed matter physics, the life and environmental sciences, and applied research. These X-rays are ideally suited for explorations of materials and biological structures; elemental distribution; chemical, magnetic, electronic states; and a wide range of technologically important engineering systems from batteries to fuel injector sprays, all of which are the foundations of our nation's economic, technological, and physical well-being. Each year, more than 5,000 researchers use the APS to produce more than 2,000 publications detailing impactful discoveries, and solve more vital biological protein structures than users of any other X-ray light source research facility. APS scientists and engineers innovate technology that is at the heart of advancing accelerator and light-source operations. This includes the insertion devices that produce extreme-brightness X-rays prized by researchers, lenses that focus the X-rays down to a few nanometers, instrumentation that maximizes the way the X-rays interact with samples being studied, and software that gathers and manages the massive quantity of data resulting from discovery research at the APS.

This research used resources of the Advanced Photon Source, a U.S. DOE Office of Science User Facility operated for the DOE Office of Science by Argonne National Laboratory under Contract No. DE-AC02-06CH11357.

Argonne National Laboratory seeks solutions to pressing national problems in science and technology. The nation's first national laboratory, Argonne conducts leading-edge basic and applied scientific research in virtually every scientific discipline. Argonne researchers work closely with researchers from hundreds of companies, universities, and federal, state and municipal agencies to help them solve their specific problems, advance America's scientific leadership and prepare the nation for a better future. With employees from more than 60 nations, Argonne is managed by UChicago Argonne, LLC for the U.S. Department of Energy's Office of Science.

The U.S. Department of Energy's Office of Science is the single largest supporter of basic research in the physical sciences in the United States and is working to address some of the most pressing challenges of our time. For more information, go to energy.gov/science.

ABOUT THE AUTHOR

Joseph E. Harmon has been a science writer, editor, and manager for four decades in several divisions within Argonne National Laboratory. He is now working as a communications manager in support of Argonne's Physical Sciences and Engineering Directorate. This article is published courtesy of Argonne National Laboratory.

THERMAL PROCESSING MEDIA PORTAL

Thermal Processing's online portal is your gateway to social media news and information resources from manufacturers and service providers in the heat-treating industry. You'll find links to social media as well as webinars, blogs and videos.

This quick-and-easy resource is just a click away at thermalprocessing.com.

Thermal processing

MARKETPLACE ///

Manufacturing excellence through quality, integration, materials, maintenance, education, and speed.

Contact **Thermal Processing** at 800-366-2185 to feature your business in the Marketplace.

ADVERTISER INDEX ///

TREVOR JONES /// PRESIDENT /// SOLAR MANUFACTURING

"Our hope is that this updated thermocouple design will be used in the heat-treat industry for those who struggle with temperature uniformity results."

Solar Manufacturing recently received a patent (#11,815,403) for an improved vacuum furnace control thermocouple design. What makes this improved design important?

Solar Manufacturing and Solar Atmospheres are required to perform temperature uniformity surveys (TUS) with all our vacuum furnaces. When surveying vacuum furnaces with smaller diameters of approximately 36 inches or less and running at lower temperatures, the surveys were not passing as easily.

There are a few things that can be done to influence results of a TUS: For example, the insertion depth of the control thermocouple in the hot zone can be adjusted. An offset can be placed into the temperature controller (which means the controller might read 1,000°, but with a 1° offset it would actually be 999°, which is permissible per AMS, within certain limits). There are also trim controls on most furnaces to adjust power to individual heating zones that affect the overall temperature uniformity of the furnace. We came up with this design development to try to alleviate those problems, therefore making the survey less burdensome.

Can you go into more detail about why the new design was developed?

After investigating this common issue, we wanted to ascertain a way to resolve it, which was spearheaded by Bill Jones. We discovered that thermal energy was being lost by means of conduction through the thermocouple and to the cold wall of the furnace. A short control thermocouple with less length to the cold wall is an exasperating natural tendency with smaller furnaces.

Knowing it was a conduction issue, we experimented with designs that could potentially resolve the issue. We found that using a smaller diameter thermocouple helped, as there was less mass to conduct the associated heat, so less energy was being lost. At this point, we knew we were on to something, but we wanted to minimize conduction even further.

There are two ceramic tubes associated with the thermocouple. One is called an inner bore and has two holes on the inside; the other tube is on the outside, called the outer sheath. Two wires, which are dissimilar metals, run parallel to the length of the inner bore as they cannot come into contact. The temperature measurement occurs at the very end, where the two wires become connected.

For this new thermocouple, we made the inner bore a single hole and had only one of the two wires going down the tube, the other running outside the tube (still not touching the other wire), which reduced the mass. To further minimize the conduction, we then segmented that bore so it was not a constant length.

The previous design was an all-alumina ceramic, which led us to look at other ceramic materials with less thermal conductivity that also maintain good temperature shock resistance. Keeping in mind that, with heating and cooling, ceramics are susceptible to breakage if there's too much of a temperature gradient, too quickly. This is called thermal shock. We found a good type of material that worked out very well for us.

Outside of the thermocouple design, we incorporated additional layers of insulation to the top side of the hot zone to further insulate the thermocouple.

What specific factors were affected by this improved design?

Temperature uniformity was the factor affected by this design — not to be confused with temperature non-uniformity. Although the furnace was still uniform throughout the working zone, the concern was that everything was running a little hotter (at temperatures of less than 1,200°F). This new thermocouple design basically shifts the overall temperature back down to where it should be.

Why is it critical to have that standard temperature uniformity?

Temperature uniformity is critical to ensure the outcome of any successful heat-treating process. Depending on who the customer is, the material you're processing, and/or the specifications you are processing to, it is a requirement to have certain levels of temperature uniformity. Generally speaking, the tighter the temperature uniformity, the more process control you're going to have, as such you are not going to have as much variability around the working zone. Typical temperature uniformity is ±10°F of the furnace setpoint; however, some requirements need to be tighter than this, and others not so stringent and can have a broader range. The level of uniformity must routinely be demonstrated and proven when running critical parts, specifically for the aerospace and medical industries.

What advantages will this new design bring to the industry as you go forward?

Our hope is that this updated thermocouple design will be used in the heat-treat industry for those who struggle with temperature uniformity results, particularly with low temperatures and smaller hot zones. Although temperature uniformity can sometimes be resolved with other "tricks," such as the insertion depth of the thermocouple or the offset or trim controls, the goal is to have a clean TUS by avoiding any of these tricks. The biggest success with this new thermocouple design is that we are now more easily passing a TUS at lower temperatures without sacrificing results across the broad range of temperatures vacuum furnaces are capable of.

MORE INFO solarmfg.com

VACUUM HEAT TREATING
FURNACES


Mentor®


Mentor® Pro


Internal and external quench


NEO™ oil quench


Vertical bottom loading


High capacity, car bottom loading

SOLUTIONS THROUGH INGENUITY

Solar Manufacturing designs and manufactures high performance, technically advanced and energy efficient vacuum heat treat furnaces. Models range from compact R&D size furnaces to mid-size horizontal production furnaces to huge car-bottom vacuum furnaces for large heavy workloads. No matter what the application or size of workload, Solar Manufacturing has the versatile, feature-rich vacuum furnace solution to fit your needs. We back it all up with outstanding Aftermarket support: spare parts, service and replacement hot zones.

SOLAR MANUFACTURING

267.384.5040
sales@solarmfg.com

solarmfg.com

Give us a call to learn more about our vacuum furnace ingenuity.